



EDITORIAL BOARD

Editor-in-Chief

B.E. Paton

Scientists of PWI, Kyiv

S.I. Kuchuk-Yatsenko (*vice-chief ed.*),

V.N. Lipodaev (*vice-chief ed.*),

Yu.S. Borisov, G.M. Grigorenko,

A.T. Zelnichenko, V.V. Knysh,

I.V. Krivtsun, Yu.N. Lankin,

L.M. Lobanov, V.D. Poznyakov,

I.A. Ryabtsev, K.A. Yushchenko

Scientists of Ukrainian Universities

V.V. Dmitrik, NTU «KhPI», Kharkov

V.V. Kvasnitsky, NTUU «KPI», Kyiv

E.P. Chvertko, NTUU «KPI», Kyiv

Foreign Scientists

N.P. Alyoshin

N.E. Bauman MSTU, Moscow, Russia

Guan Qiao

Beijing Aeronautical Institute, China

M. Zinigrad

Ariel University, Israel

V.I. Lysak

Volgograd STU, Russia

Ya. Pilarczyk

Welding Institute, Gliwice, Poland

U. Reisgen

Welding and Joining Institute, Aachen, Germany

G.A. Turichin

St. Petersburg SPU, Russia

Founders

E.O. Paton Electric Welding Institute, NASU

International Association «Welding»

Publisher

International Association «Welding»

Translators

A.A. Fomin, O.S. Kurochko, I.N. Kutianova

Editor

N.G. Khomenko

Electron galley

D.I. Sereda, T.Yu. Snegiryova

Address

E.O. Paton Electric Welding Institute,

International Association «Welding»

11 Kazimir Malevich Str. (former Bozhenko Str.),

03150, Kyiv, Ukraine

Tel.: (38044) 200 60 16, 200 82 77

Fax: (38044) 200 82 77, 200 81 45

E-mail: journal@paton.kiev.ua

www.patonpublishinghouse.com

State Registration Certificate

KV 4790 of 09.01.2001

ISSN 0957-798X

DOI: <http://dx.doi.org/10.15407/tpwj>

Subscriptions

\$348, 12 issues per year,

air postage and packaging included.

Back issues available.

All rights reserved.

This publication and each of the articles contained

herein are protected by copyright.

Permission to reproduce material contained in this journal must be obtained in writing from the Publisher.

CONTENTS

Avtomaticheskaya Svarka Journal is 70 2

SCIENTIFIC AND TECHNICAL

Poznyakov V.D. Weldability of high-strength alloyed steels with yield strength of 590–785 MPa 6

Tsybulkin G.A. Effect of own magnetic fields on electric arcs in tandem-arc welding 12

Degtyarev V.A. Fatigue resistance of steel welded joints of different strength with steady residual stresses 16

Schwab S.L., Petrychenko I.K. and Akhonin S.V. Influence of rare-earth elements on the structure and properties of welds of VT22 titanium alloy 20

Razmyshlyayev A.D. and Ageeva M.V. On mechanism of weld metal structure refinement in arc welding under action of magnetic fields (Review) 25

INDUSTRIAL

Majdanchuk T.B., Ilyushenko V.M. and Bondarenko A.N. Influence of arc surfacing modes on intergranular penetration of high-tin bronze into steel 29

Kuskov Yu.M., Soloviov V.G., Osechkov P.P. and Osin V.V. Electroslag surfacing with large-section electrode at direct current in current-supplying mould 32

Panteleymonov E.A. On the problem of heat treatment of welded joints of railway rails 36

Burlaka V.V., Gulakov S.V. and Podnebenna S.K. AC arc stabilizer for welding transformers 40

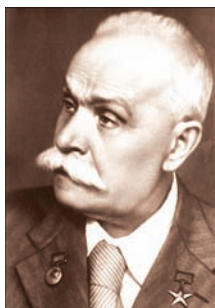
INFORMATION

Poland Institute of Welding In Gliwice 43

Welding of Titanium and its Alloys 46

Microplasma Spraying of Biocompatible Coatings on Implants 47

Avtomaticheskaya Svarka Journal is 70



March, 1948 is believed to be the time of birth of the Journal, when the first issue of the collection «Transactions on Automatic Submerged-Arc Welding» was published.

Academician Evgeny Oscarovich Paton was the initiator of its publication. The collection publication became systematic and in June, 1950 it was transformed into «Avtomaticheskaya Svarka» (Automatic Welding) Journal — a monthly publication of the E.O. Paton Electric Welding Institute.



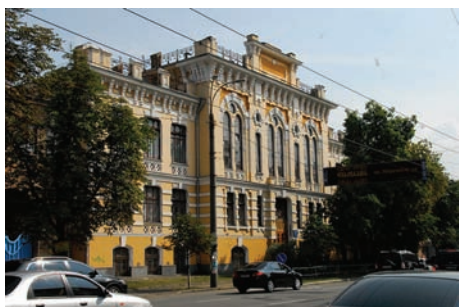
Appearance of collections, and then also of the Journal was preceded by issue of individual brochures on the topics of the work of the Electric Welding Laboratory, and then also the Electric Welding Institute. Academician E.O. Paton always attached great importance to operative scientific and technical information. The new specialized periodical was created with the purpose of regular coverage of research results and experience of practical application of the rapidly developing technologies of welding metallic materials. Compared to regular academic journals it featured broad coverage of the considered problems — from deep scientific research up to practical application of their results in various branches of the national economy.

Appearance of «Avtomaticheskaya Svarka» Journal immediately attracted the attention of all those interested in welding, and specialists of not only PWI, but also many other USSR research institutes, plants and enterprises become its authors.

From 1959 till 1986 the English version of «Avtomaticheskaya Svarka» Journal was published by the British Welding Institute under «Automatic Welding» title. In the period from 1991 till 1999 the Journal was reedited in Great Britain by private publisher Rieckansky under the title «The Paton Welding Journal». Since 2000 its publication at PWI under the same title was organized.

During the first several years the Journal, in keeping with its title, published predominantly the investigation results and experience of application of automatic submerged-arc welding. The fundamentals of the theory of welding and welded structures were established taking this technological process as an example. At the same time, starting from the very first issues, other welding processes, as well as related processes, were given due attention on its pages. However, even later the Journal retained its initial title of «Avtomaticheskaya Svarka», as a tribute to the tradition established by its founder Evgeny Oscarovich Paton.

During these years papers, devoted to study of the causes for brittle fracture, evaluation of weldability of carbon and low-alloyed steels, non-ferrous metals and alloys, were published. These and subsequent studies led to formation of scientific ideas about welding as a metallurgical process, substantiation of the need to develop new structural steels and alloys, allowing for process and metallurgical features of welding.



The Journal covered the work on fundamentals of the theory of automatic regulation, considering the arc power source, consumable electrode, feed mechanism and the arc as one system; on creation of equipment for mechanized welding processes. After the death of E.O. Paton in August,



1953, the Editorial Board was headed by Boris Evgenievich Paton. During the subsequent years the range of publication subjects was widened. In particular, the Journal started publishing information about application of welding heat sources to produce super high quality metallic materials. This second main scientific direction of PWI activity has been covered in another publication of the Institute since 1960s — «Problemy Sovremennoj Elektrometallurgii» Journal (now «Sovremennaya Elektrometallurgiya»).

Starting from 1960s, in connection with the fact that PWI was entrusted with the functions of the head organization on welding and special electrometallurgy in the USSR, the Coordination Council on Welding, Scientific Council of USSR SCST, and Scientific Council of USSR

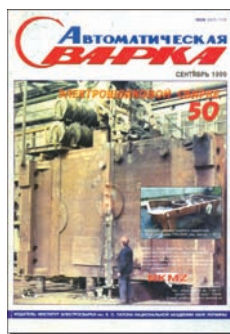
AS were set up at the Institute. The Journal started publishing materials on organization of welding production, coordination of scientific research, problems of information, training welding specialists, etc.

Journal publications had considerable influence on development of fabrication of welded structures and products for power, heavy and chemical engineering, in industrial construction, rocket-, shipbuilding, railway and pipeline transportation, tank building, radio electronics and many other fields of modern engineering.

Reflecting the results of achievements of PWI and other organizations, the Journal was the first in the world to highlight many outstanding developments and followed-up their progress. The following should be regarded as such developments:



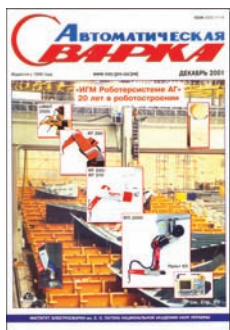
Space Technologies



Electroslag Welding



Plasma Technologies



Laser Technologies



Pressure Welding



Explosion Welding

- arc welding with forced formation of the weld, allowing application of mechanized welding in site;

- electroslag welding, which allows producing single-pass joints of items of practically unlimited wall thickness, and which was the base for one of the new metallurgical processes — electroslag remelting;

- technology of sheet structure fabrication by coiling;

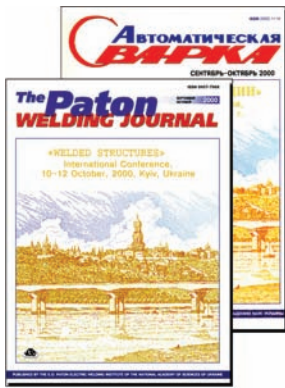
- technology of fabrication of multilayer structures;

- technology of fabrication of forge-welded and cast-welded structures;

- CO₂ welding with small-diameter wire as one of the most widely accepted methods of mechanized welding up to now;

- welding over activating flux and with activated wire;

Proceedings of the International Conferences



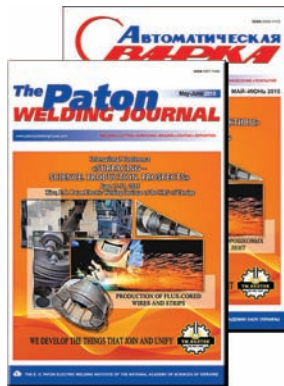
Welded Structures



Current Problems in Welding



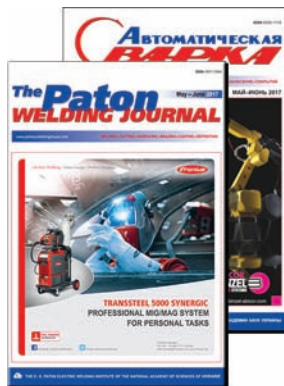
Welding Consumables



Surfacing. Science.
Production. Prospects



Modern Welding
Technologies



Robotization and
Automation

- consumable electrode pulsed-arc welding, which is especially effective in manufacturing aluminium alloy products;
- multielectrode arc welding into a common pool which became the main technology in industrial production of large-diameter pipes;
- continuous flash-butt welding of rails, pipes and other items of a large cross-section, which allows solving a number of complex and important engineering problems;
- electron beam welding which turned out to be highly efficient in fabrication of critical thick-walled items;
- vapour-phase technologies with electron beam heating;
- microplasma welding — for items of thickness from hundredth of a millimeter up to 1 mm;
- underwater mechanized welding in «wet» variant;
- plasma cutting;
- explosion welding and cutting;
- technology of manufacturing cryogenic engineering products based on modern high-alloyed steels;
- welding in space;
- electric arc surfacing with alloys improving service properties of items;
- welding of dissimilar composite materials;
- plasma and thermal spraying of protective and other materials on products.

The Journal systematically publishes the results of studying the physical features of diverse phenomena occurring in the molten metal; application of various heat sources; studying the interaction of molten metal with gases and slags, as a base for creation of efficient welding consumables; hygiene and labour safety in welding production.

On the pages of «Avtomaticheskaya Svarka» Journal one can find extensive information about welding processes and properties of welded joints of alloys based on iron, aluminium, copper, nickel, titanium, niobium and other metallic materials, as well as plastics, ceramics, etc. The breadth of factual data and depth of investigation of the structure and properties of various materials allow us to consider the Journal not only a welding, but also a materials science publication.

Many published articles reflect the results of studying the residual stresses and strains, as well as the methods to reduce them. The Journal regularly publishes articles on the subject of strength of welded joints and structures. This work resulted in development of efficient methods of determination and controlling the stress-strain states, methods of flaw detection and diagnostics of welded structures. At present developments related to monitoring and diagnostics of diverse weldments, are published in one more PWI Journal — «Tekhnicheskaya Diagnostika i Nerazrushayushchij Kontrol», issued since 1989.

It should be noted that in 1960s and 1970s the number of publications devoted to development of new and improvement of traditional kinds of welding consumables — electrodes, wires, fluxes, and organization of their mass production, has greatly increased in the Journal.

During the same period, the Journal systematically published articles on automatic control of welding processes, many of which can be regarded as pioneering, as well as investigation of power systems and peculiarities of design of electric welding machines. Readers are regularly provided with information on development of new samples of welding equipment and consumables.

Information about coating processes, coating properties, and development of materials required for this purpose, appears more and more often on the Journal pages.

Journal circulation during these years reached 8000 copies. It is received on a subscription basis in many countries of the world.

In 1992 «Avtomaticheskaya Svarka» acquired the status of international scientific-technical and production journal. Its editorial board includes leading specialists from Germany, Israel, China, Poland and RF.

In the new millennium «Avtomaticheskaya Svarka» Journal, similar to many other scientific journals, is going through difficult times, but it still continues to act as the initiator of qualified informing of welding production specialists about the status and development of individual technologies of welding production. Thematic issues of the Journal in the areas of «Electroslag Welding» (No.9, 1999), «Space Technologies» (No.10, 1999), «Plasma Technologies» (No.12, 2000), «Laser Technologies» (No.12, 2001), «Pressure Welding» (No.7, 2002), «Explosion Welding» (No.11, 2009) are published, as well as Journal issues which are the proceedings of International Conferences on «Welded Structures» (Nos 9–10, 2000), «Current Problems in Welding and Life of Structures» (Nos 10–11, 2003), «Welding Consumables» (Nos 6–7, 2014), «Surfacing. Science. Production. Prospects» (Nos 5–6, 2015), «Modern Welding Technologies» (Nos 5–6, 2016), and «Robotization and Automation of Welding Processes» (Nos 5–6, 2017). Individual issues of the Journal contain selections of articles of scientists and lecturers, devoted to jubilees of welding departments and profile chairs of technical universities of Ukraine. The Journal describes best practices and major developments of leading West European and US companies, many of which founded subsidiary companies in Ukraine in this period.

Over the 70 years the Journal has published more than 12 thousand papers, dealing with different problems of welding production and all the aspects of the science of welding, as well as many problems of related technologies. A wide range of publications added up into a kind of chronicle, which allows judging the achievements and dynamics of development of welding science and technology over the 70 years. By the breadth and depth of coverage of the highlighted topics, the Journal issues can be considered a welding encyclopedia. The information contained in this publication has served and continues to serve scientific and technical progress.

At present «Avtomaticheskaya Svarka» Journal is presented in INSPEC (Great Britain), EBSCO (USA), Weldasearch Select (France) databases; Google Scholar (USA); Dzhirelo (Ukraine), Svarka (Russia), Welding Abstracts (Great Britain) abstract journals; it is abstracted in Rivista Italiana della Saldatura (Italy); highlighted in reviews in Japanese Journal of Light Metal Welding, Journal of the Japan Welding Society, Quarterly Journal of the Japan Welding Society, Journal of Japan Institute of Metals, and Welding Technology journal. Starting from 2016 Journal articles are included into CrossRef, and are assigned DOI index (Digital Object Identifier). An urgent goal at the modern stage is Journal inclusion into international scientometric bases. The archive of articles from «Avtomaticheskaya Svarka» Journal in Russian and in English has been open access on the Journal web-site [www.patonpublishinghouse.com/rus\(eng\)/journals/as](http://www.patonpublishinghouse.com/rus(eng)/journals/as) since 2000.

Welding processes in the third millennium still remain a key technology of joining materials and creating structures. They will be further improved through development of high-efficient automated and robotic energy-saving technologies. And «Avtomaticheskaya Svarka» professional Journal will still have an important role of informational support of welding production professionals.

Journal Editorial Board

WELDABILITY OF HIGH-STRENGTH ALLOYED STEELS WITH YIELD STRENGTH OF 590–785 MPa

V.D. POZNYAKOV

E.O. Paton Electric Welding Institute of the NAS of Ukraine
11 Kazimir Malevich Str., 03150, Kyiv, Ukraine. E-mail: office@paton.kiev.ua

This paper summarizes the results of investigations of influence of the thermal cycles, characteristic for arc welding processes, on the structure and mechanical properties of high-strength alloyed steels with yield strength of 590–785 MPa, as well as on their susceptibility to cold crack formation. The structural transformations in the metal of heat-affected-zone of welded joints were investigated using a quick-response dilatometer, and its mechanical properties and susceptibility to cold crack formation were evaluated according to the results of tests of standard specimens and by the Implant method, respectively. The diagrams of the structural transformations of austenite in the region of metal overheating of heat-affected-zone of a number of high-strength alloyed steels, the dependences of change in their mechanical properties during welding, and also the data, characterizing the susceptibility of high-strength alloyed steels to cold crack formation at different concentrations of diffusion hydrogen in the deposited metal, are presented. 15 Ref., 4 Tables, 4 Figures.

Keywords: *high-strength steels, arc welding, metal structure, mechanical properties, cold cracks*

The many year experience in application of high-strength alloyed steels with a yield strength of 590–785 MPa in welded structures is the evidence of their high technical and economic efficiency. Such structures are reliable in service under the most severe operating conditions, not only at static loads, but also at impact loads.

These steels found the most wide application in machine building in the manufacture of highly-loaded structure elements, among which there are mine supports and skips, arrows of cranes and concrete pumps, bodies of large-tonnage dump trucks, beam-arms, arrows, swinging circles and buckets of excavators.

A distinctive feature of high-strength alloyed steels (Tables 1, 2) is the fact that except of a remarkably high strength, they are characterized by high impact strength at a lower temperature. This is achieved due to rational alloying of steels with manganese, nickel, chromium, molybdenum, microalloying with boron, vanadium, aluminum, niobium and heat treatment, which consists of quenching to martensite from the temperature of 900–950 °C and high tempering at the temperature of 600–680 °C [1]. A particularly high cold resistance is in high-strength resistant steels with low sulfur and phosphorus content. To produce such steels at metallurgical enterprises the electroslag remelting (ESR), blowing with argon, treatment with synthetic slags [2, 3] or other measures are used, providing the efficient purification of molten metal from harmful impurities. To such steels the steels

12GN2MFAYU-Sh and 12GN3MFAUYDR-Sh belong, given in the Tables 1 and 2.

The disadvantage of high-strength steels is their susceptibility to cold crack formation [4–7]. This is connected with the fact that during the process of welding a low-plastic brittle martensitic structure can form in the metal of heat-affected-zone (HAZ) of welded joints. The process of cold crack formation is intensified by diffusion hydrogen, which enters the weld pool with the molten metal.

Unlike the steel rolled metal, the metal structure of which depends mainly on the chemical composition, the method and mode of heat treatment, the formation of the structure of HAZ metal of welded joints of high-strength alloyed steels is also affected by the thermal cycle of welding (TCW) [8–12]. The most significant changes in the structure of steel during welding occur in the region of overheating of HAZ metal, i.e., in that region which is located in the direct vicinity of the weld and is heated up to the temperatures of 1300–1150 °C.

The aim of this work consisted in generalizing the results of investigations carried out at the E.O. Paton Electric Welding Institute, directed to studying the influence of thermal cycles, characteristic for arc welding processes, on the structure and mechanical properties of HAZ metal of high-strength alloyed steels with a yield strength of 590–785 MPa, as well as on their susceptibility to cold crack formation depending on the conditions of cooling of welded joints and the content of diffusion hydrogen in the deposited metal.

Table 1. Requirements to chemical composition of high-strength alloyed steels, wt.%

Steel	C	Si	Mn	Cr	Ni	Mo
12GN2MFAYu	0.09–0.16	0.3–0.5	0.9–1.2	0.2–0.5	1.40–1.75	0.15–0.25
12GN2MFAYuSh	0.09–0.16	0.3–0.5	0.9–1.2	0.2–0.5	1.40–1.75	0.15–0.25
14KhG2SAFD	0.12–0.18	0.4–0.7	1.4–1.9	0.5–0.8	<0.3	–
14Kh2GMR	0.10–0.16	0.17–0.37	0.9–1.2	1.1–1.5	<0.3	0.4–0.5
12GN3MFAYuDR-Sh	0.10–0.15	0.17–0.37	1.2–1.5	–	2.8–3.0	0.3–0.4
14KhGN2MDAFB	0.12–0.17	0.17–0.37	1.1–1.4	0.9–1.3	1.7–2.2	0.2–0.3

Table 1 (cont.)

Steel	Cu	V	Nb	B	Al	S	P
12GN2MFAYu	<0.3	0.05–0.10	–	–	0.05–0.10	≤0.035	≤0.035
12GN2MFAYuSh	<0.3	0.05–0.10	–	–	0.05–0.10	≤0.010	≤0.020
14KhG2SAFD	0.3–0.6	0.08–0.16	–	–	0.03–0.07	≤0.02	≤0.035
14Kh2GMR	0.20	<0.3	0.01–0.04	0.001–0.004	0.02–0.08	≤0.035	≤0.035
12GN3MFAYuDR-Sh	0.3–0.5	0.04–0.08	–	–	0.02–0.05	≤0.010	≤0.020
14KhGN2MDAFB	0.3–0.6	0.10–0.20	0.03–0.08	–	0.03–0.10	≤0.008	≤0.020

In arc welding, the TCW parameters depend on many factors. The most important among them are the input energy of welding, the initial temperature of the metal and its thickness. With the increase in the input energy and the initial temperature of steel, the period of staying HAZ metal in the temperature range of 800–500 °C ($t_{8/5}$) increases, and its cooling rate in the temperature range of 600–500 °C ($w_{6/5}$) decreases. With an increase in the metal thickness, these values, on the contrary, decrease and increase, respectively. Depending on this fact, the structure and, consequently, the mechanical properties of HAZ metal are changed.

To determine the effect of the chemical composition and the conditions of cooling the metal on its structure, the diagrams of austenite transformation are usually used, which are plotted with account for the processes occurring in arc welding. In order to provide a high resistance of austenite, characteristic for welding, as the standard for plotting the diagrams, such conditions for heating the specimens (w_h) are selected at which the individual features of steels began to be sufficiently clearly manifested with respect to the susceptibility to grains growth. The cooling rate of dilatometric specimens is selected, coming from the need to provide such conditions in the range of temperatures of the lowest stability of austenite, which

will be as close as possible to the cooling conditions of HAZ metal of welded joints [13]. To simulate the conditions, typical for arc welding processes, the heating rate of the specimens is set in the range of 150–180 °C/s.

The heating rate of the specimens is controlled by changing the value of the current passing through the specimen according to the set program, and the rate of cooling is controlled by passing water through the devices in which the specimen is fixed, blowing the specimens with inert gas or by passing a low current through them.

The diagrams, characterizing the transformations of austenite in HAZ metal of high-strength alloyed steels during continuous cooling of specimens according to the thermal cycle of welding are shown in Figure 1. The chemical composition and mechanical properties of the investigated steels are given in Tables 3 and 4.

The typical characteristic for the considered high-strength alloyed steels is that the formation of martensite in them begins at the relatively low cooling rates ($w_{6/5} = 2–4$ °C/s). With increase in $w_{6/5}$, the amount of martensite in HAZ metal of such steels increases. This occurs more sharply in steels 14Kh2GMR, 12GN3MFAYuDR-Sh and 14KhGN2MDAFB. At

Table 2. Requirements to mechanical properties of high-strength alloyed steels (not less than)

Steel	$\sigma_{0.2}$	σ_t	δ_5	KCU_{-40}	KCV_{-40}
	MPa		%	J/cm ²	
12GN2MFAYu	590	690	14	29	–
12GN2MFAYuSh	590	690	14	–	39
14KhG2SAFD	590	690	14	39	–
14Kh2GMR	590	690	14	39	–
12GN3MFAYuDR-Sh	685	780	16	–	39
14KhGN2MDAFB	785	885	15	39	–

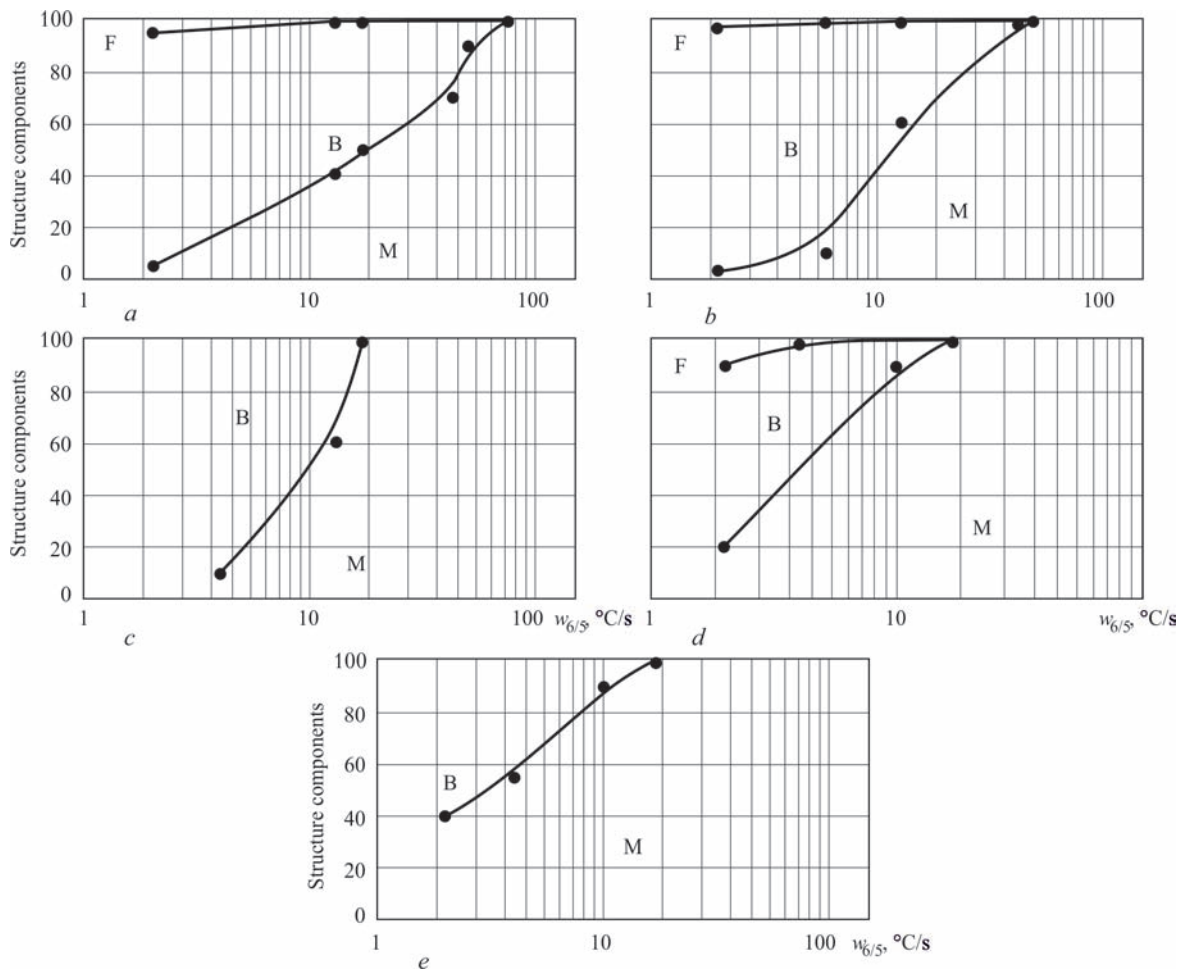


Figure 1. Diagrams of structural transformations of austenite in the overheating region of HAZ metal of high-strength alloyed steels 12GN2MFAYu (a), 14KhG2SAFD (b), 14Kh2GMR (c), 12GN3MFAYuDR (d) and 14KhGN2MDAFB (e)

$w_{6/5} = 4-8$ °C/s the amount of martensite in the structure of HAZ metal of these steels reaches 50 %, and at $w_{6/5} = 20$ °C/s — 100 %. In steels 12GN2MFAYu and 14KhG2SAFD, martensite in the amount of 50 % is formed at the higher cooling rates, $w_{6/5} = 20$ and 14 °C/s, respectively, and 100 % of martensite in them is observed at $w_{6/5} = 70$ and 50 °C/s. Moreover, it should

be noted that as compared to high-strength alloyed steels of other grades, in steel 12GN3MFAYuDR-Sh the martensitic transformation are finished at the lower temperatures (200–250 °C). The mentioned factors, as is known, can have a significant effect on mechanical properties of HAZ metal of welded joints and their resistance to cold crack formation.

Table 3. Chemical composition of the investigated high-strength alloyed steels, wt. %

Steel	C	Si	Mn	Cr	Ni	Mo	Cu	V	Nb	Ti	Al	S	P
12GN2MFAYu	0.15	0.41	1.14	0.38	1.56	0.22	0.19	0.07	–	–	0.06	0.032	0.014
14KhG2SAFD	0.13	0.57	1.42	–	–	–	0.39	0.08	–	–	0.08	0.015	0.019
14Kh2GMR	0.15	0.28	1.10	1.30	–	0.43	0.20	–	0.02	–	0.05	0.023	0.024
12GN3MFAYuDR	0.13	0.23	1.36	–	3.08	0.33	0.40	0.05	–	–	0.02	0.004	0.020
14KhGN2MDAFB	0.14	0.25	1.30	1.15	1.94	0.24	0.42	0.14	0.04	–	0.05	0.008	0.014

Table 4. Mechanical properties of the investigated high-strength alloyed steels

Steel	$\sigma_{0.2}$	σ_t	δ_5	ψ	KCU_{-40}	KCU_{-40}
	MPa		%		J/cm ²	
12GN2MFAYu	625	720	20.8	62.2	80	52
14KhG2SAFD	635	750	20.0	54.3	65	52
14Kh2GMR	680	780	18.1	55.3	55	48
12GN3MFAYuDR-Sh	821	887	19.2	52.6	186	130
14KhGN2MDAFB	860	920	17.3	60.0	120	64

Taking into account that the structure of separate regions of HAZ metal of welded joints is not homogeneous, and the sizes of these regions are extremely small, the model specimens of 150×13×13 mm size were used to determine the effect of cooling conditions on mechanical properties of HAZ overheating region. The same as in dilatometric investigations, they were forcibly heated and cooled as to thermal welding cycles in accordance with the procedure, described in the work [14].

The rate of heating the specimens up to the temperature of 1350 °C was controlled with the help of a programming device of the installation MSR-75, and the cooling rate $w_{6/5}$ was changed from 2.7 to 50 °C/s by using the forced air cooling with different intensity.

To determine the effect of arc welding processes on mechanical properties of the overheating region of HAZ metal of the mentioned steels the specimens for tensile tests (type II according to GOST 6996–66) and impact bending (type VIII and type XI according to GOST 6996–66) were manufactured from the billets treated by TCW. The tensile tests of specimens were carried out at the temperature of 20 °C, and the tests on impact bending were carried out at the temperature of –40 °C. Their results are shown in Figures 2 and 3.

As follows from Figure 2, under the influence of TCW, the impact toughness of the metal in HAZ over-

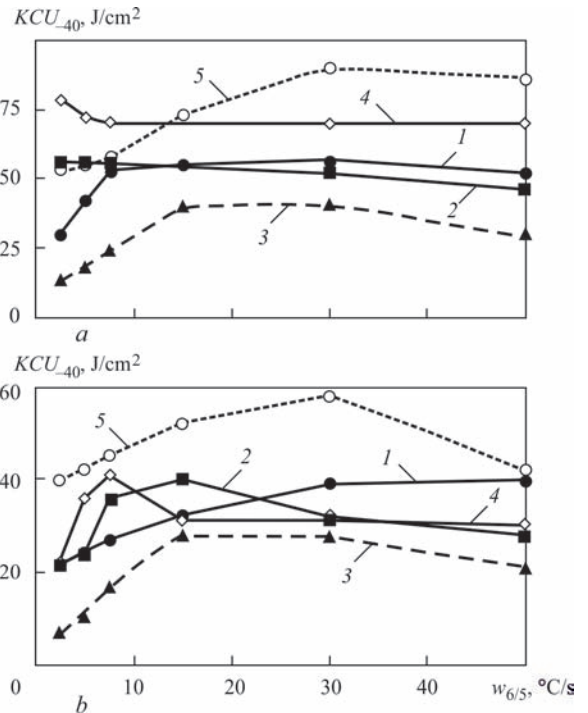


Figure 2. Influence of cooling rate $w_{6/5}$ on KCU_{-40} (a) and KCU_{-40} (b) of metal in the region of overheating of HAZ of steels: 12GN2MFAYu (1), 14Kh2GMR (2), 14KhG2SAFD (3), 14KhGN2MDAFB (4), 12GN3MFAYuDR-Sh (5)

heating region relative to the initial state of the steel is reduced. But, despite this, at $w_{6/5} > 5$ °C/s, these values for most of the investigated high-strength alloyed

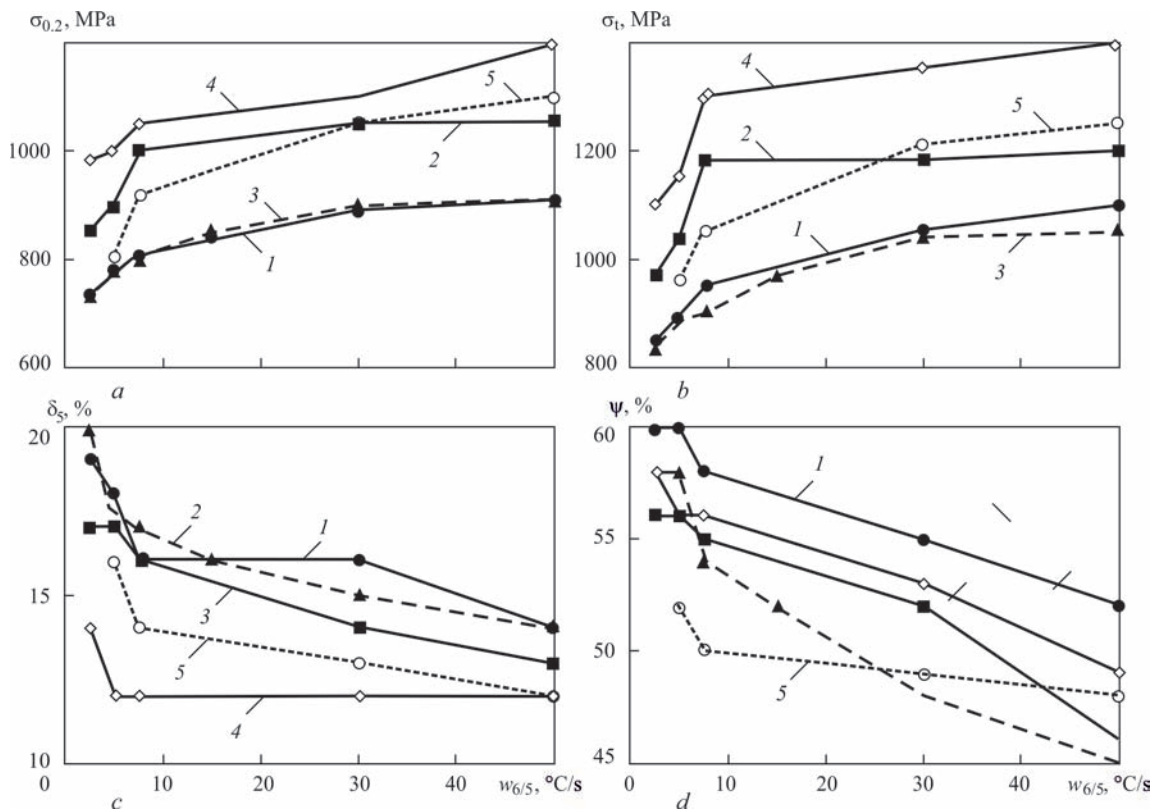


Figure 3. Influence of cooling rate $w_{6/5}$ on the values of yield strength (a), tensile strength (b), relative elongation (c) and reduction in region (d) of metal in the region of overheating of HAZ of steels: 12GN2MFAYu (1), 14Kh2GMR (2), 14KhG2SAFD (3), 14KhGN2MDAFB (4), 12GN3MFAYuDR-Sh (5)

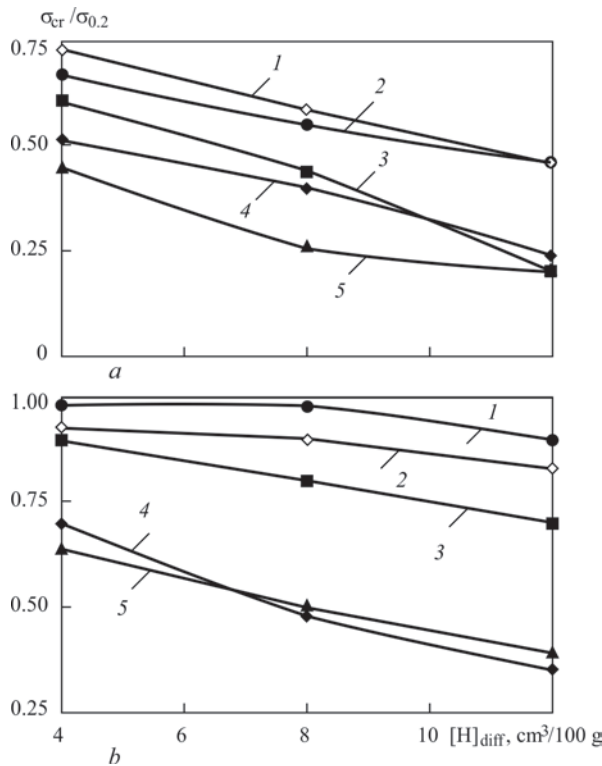


Figure 4. Resistance of steels 12GN2MFAYu (1), 12GN3MFAYuDR (2), 14KhG2SAFD (3), 14KhGN2MDAFB (4), 14Kh2GMR (5) to cold crack formation depending on the content of diffusion hydrogen in the deposited metal and the conditions of cooling HAZ metal: *a* — $w_{6/5} = 25$ °C/s; *b* — 10

steels are at the level of the requirements specified to steel rolled metal. The exception is the steel of grade 14KhG2SAFD. The required level of impact toughness values in HAZ metal of welded joints of the mentioned steel can be obtained only in that case when welding is performed at the modes which provide its cooling at a rate of $w_{6/5} = 15\text{--}30$ °C/s.

The graphical material shown in Figure 3, indicates that with increase in the cooling rate, the values of yield strength and the tensile strength of the metal in the overheating region of HAZ are firstly sharply increased, and then increase monotonically. The elongation and relative reduction in area decrease. This is quite natural, since, as was indicated above, as the cooling rate in the metal increases, the amount of the martensitic component increases, and the martensite, as is known, has a high strength, but also has a low ductility.

The evaluation of susceptibility of high-strength alloyed steels to cold crack formation was carried out according to the Implant method. The effect of the diffusion hydrogen content ($[H]_{\text{diff}}$) and the cooling rate of welded joints on the resistance of steels to cold crack formation was studied. The specimens-implants of 6 mm diameter with a stress concentrator in the form of a spiral groove were used. The welding of specimens installed in the holes of the base plate

of 20 mm thickness was performed by the electrodes of grade ANP-9 (type E85) of 4 mm diameter at the mode: $I_w = 160\text{--}170$ A; $U_a = 25\text{--}26$ V; $v_w = 8.5\text{--}9.0$ m/h. The loading of specimens was started during cooling at the temperature of 150–100 °C.

The rate of HAZ metal cooling $w_{6/5}$ from 25 to 10 °C/s was regulated by the preheating temperature of base plates, which in its turn was selected according to the oscillograms of thermal welding cycles for high-temperature regions of HAZ of specimens-implants. The cooling rate of HAZ metal at the level of 25 °C/s was obtained during welding without preheating, and at 10 °C/s it was obtained during preheating of base plates to the temperature of 120 °C. The amount of diffusion hydrogen in the deposited metal depended on the temperature and the time of calcination of electrodes and varied from 4 to 12 cm³/100 g. Its content was determined by the chromatographic method [15].

Since HAZ metal of the investigated high-strength steels has a different static strength, as a criterion characterizing its resistance to cold crack formation, a dimensionless value was used, namely the ratio $\sigma_{\text{cr}}/\sigma_{0.2}$, where $\sigma_{0.2}$ is the conditional yield strength of HAZ metal, which it possesses under the specific welding conditions (cooling of welded joints), and σ_{cr} is the critical (maximal) value of stresses, which the specimens are able to withstand without crack formation.

The results of testing the specimens using the Implant method (Figure 4) prove that at the content of diffusion hydrogen in the deposited metal, limited to 4 cm³/100 g, the HAZ metal of welded joints of high-strength alloyed steels of type 12GN2MFAYu and 12GN3MFAYuDR-Sh is distinguished by a high resistance to cold crack formation. It is shown by the fact, that even in the case when welding is carried out without preheating ($w_{6/5} = 25$ °C/s), the value $\sigma_{\text{cr}}/\sigma_{0.2}$ of these steels is in the range of 0.7–0.75. The susceptibility of steels of grades 12GN2MFAYu and 12GN3MFAYuDR-Sh to cold crack formation, as well as of other high-strength alloyed steels, is pronounced and intensified with increase in content of $[H]_{\text{diff}}$ in the deposited metal.

To reduce the risk of cold crack formation in welded joints of high-strength alloyed steels of grades 14Kh2GMR, 14KhGN2MDAFB and 14KhG2SAFD, it is necessary not only to considerably limit the content of diffusion hydrogen in the deposited metal, but also to preheat them to the temperature of not lower than 120 °C.

Conclusions

1. High-strength alloyed heat-hardened steels combine the high strength and cold resistance.

2. Under the influence of thermal cycles, characteristic for arc welding processes, the transformation of austenite in HAZ metal of the considered high-strength alloyed steels occurs in the bainite and martensite regions.

3. The increase in cooling rate of HAZ metal of high-strength alloyed steels causes improvement in the strength properties ($\sigma_{0.2}$ and σ_T), however it decreases its ductility (δ_5 and ψ).

4. To produce welded joints of high-strength steels with the required complex of mechanical properties and sufficient resistance to cold crack formation the content of diffusion hydrogen in the deposited metal should not exceed 4 cm³/100 g and the modes of welding and the temperature of preheating should be selected in such a way that they could provide the cooling rate of HAZ metal in the range of 5–20 °C/s.

1. Show, B.K., Veerababu, R., Balamuralikrishnan, R., Malakondaiah, G. (2010) Effect of vanadium and titanium modification on the microstructure and mechanical properties of microalloyed HSLA steel. *Mater. Sci. Eng., A*, **527**, 1595–1604.
2. Paton, B.E., Medovar, B.I., Tikhonov, V.A. et al. (1984) Examination of possibility of quality improvement of thick-sheet high-strength structural steels 12GN2MFAYu (VS-1) and 12Kh2MFBAYu (VS-2) using electroslag remelting method. *Problemy Spets. Elektrometallurgii*, **21**, 3–7 [in Russian].
3. Paton, B.E., Medovar, B.I., Tikhonov, V.A. et al. (1985) Electroslag remelting of high-strength structural steels 12GN2MFAYu (VS-1) grade under fluxes containing rare-earth metals. *Ibid.*, **1**, 5–7 [in Russian].
4. Pokhodnya, I.K., Shvachko, V.I. (1996) Cold cracks welded joint of structural steels. *Materials Sci.*, **32(1)**, 45–55.
5. Stevenson, M.E., Slowrie, S.L., Bowman, R.D., Bennett, B.A. (2002) Metallurgical failure analysis of cold cracking in a structural steel weldment: Revisiting a classic failure mechanism. *Practical Failure Analysis*, **2**, 55–60.
6. Garasic, I., Coric, A., Kozuh, Z., Dzic, I. (2010) Occurrence of cold cracks in welding of high-strength S960 QL steel. *Technical Gazette*, **17**, 327–335.
7. Lobanov, L.M., Poznyakov, V.D., Makhnenko, O.V. (2013) Formation of cold cracks in welded joints from high-strength steels with 350-850 MPa yield strength. *The Paton Welding J.*, **7**, 7–12.
8. Keehan, E., Zachrisson, J., Karlsson, L. (2010) Influence of cooling rate on microstructure and properties of high strength steel weld metal. *Sci. and Techn. of Welding and Joining*, **15**, 233–238.
9. Svensson, L.-E. (2007) Microstructure and properties of high strength weld metals. *Materials Sci. Forum*, **539–543**, 3937–3942.
10. Ragu Nathan, S., Balasubramanian, V., Malarvizhi, S., Rao, A.G. (2015) Effect of welding processes on mechanical and microstructural characteristics of high strength low alloy naval grade steel joints. *Defence Technology*, **11(3)**, 308–317.
11. Ghazanfari, H., Naderi, M. (2013) Influence of welding parameters on microstructure and mechanical performance of resistance spot welded high strength steels. *Acta Metall. Sin.*, **26(5)**, 635–640.
12. Ghazanfari, H., Naderi, M., Iranmanesh, M., Seydi, M. (2012) A comparative study of the microstructure and mechanical properties of HTLA steel welds obtained by the tungsten arc welding and resistance spot welding. *Materials Sci. and Engineering*, **534**, 90–100.
13. Shorshorov, M. Kh., Belov, V.V. (1972) *Phase transformations and changes of steel properties in welding*. Moscow, Nauka [in Russian].
14. Sarzhevsky, V.A., Sazonov, V.Ya. (1981) Unit for simulation of welding thermal cycles based on the machine MSR-75. *Avtomatich. Svarka*, **5**, 69–70 [in Russian].
15. Pokhodnya, I.K., Paltsevich, A.P. (1980) Chromatographic method for determination of diffusion hydrogen amount in welds. *Ibid.*, **1**, 37–39 [in Russian].

Received 08.02.2018

EFFECT OF OWN MAGNETIC FIELDS ON ELECTRIC ARCS IN TANDEM-ARC WELDING

G.A. TSYBULKIN

E.O. Paton Electric Welding Institute of the NAS of Ukraine
11 Kazimir Malevich Str., 03150, Kyiv, Ukraine. E-mail: office@paton.kiev.ua

Considered is an effect of own magnetic fields on spatial position of arcs appearing in their deviation from electrode axial lines in automatic tandem-arc welding. The main aim of work is obtaining the dependencies of indicated deviations from arc lengths and welding currents in analytical form. In scope of this problem the conditions were found that limit a relationship between welding currents. Their neglecting can result in «adhesion» of arcs or their extinction in process of welding. In particular, the relationship between height («amplitude») of welding current pulse of one arc and basic current of another one should not exceed specific limit in pulse tandem-arc consumable electrode welding. The work is illustrated by the examples. 9 Ref., 1 Figure.

Keywords: *tandem-arc welding, consumable electrode, electromagnetic interaction of arcs*

Due to recent achievements in the field of design of welding current sources with microprocessor control there is a possibility to realize automatic arc welding with two successive arcs in shielding gas (Tandem Welding). According to work [1] the main advantage of tandem-arc welding in comparison with welding using one arc is significant increase of its efficiency.

From technical point of view the tandem welding is sufficiently complex process requiring coordinated control of welding with both arcs burning in the vicinity to each other. Besides, the undesirable arc deformations can appear due to close positioning of the electrodes. This can result in their «adhesion» or extinction in process of welding. The main reason of the indicated deformations is electromagnetic interaction of parallel arcs with currents. The forces of this interaction, as it is known, are determined by Ampere law

$$F_{12} = \frac{\mu_0 \mu}{2\pi} \frac{i_1 i_2}{r} l_2, \quad F_{21} = \frac{\mu_0 \mu}{2\pi} \frac{i_1 i_2}{r} l_1. \quad (1)$$

In formulae (1) F_{12} is the force acting the second arc from the side of the first arc; F_{21} is the force acting the first arc from the side of the second; μ_0 is the magnetic constant; μ is the relative magnetic permeability of the medium; i_1, i_2 are the welding currents of the first and second arcs; l_1, l_2 are the lengths of the first and second arcs; r is the distance between the arcs.

The welding arcs with similarly oriented currents will curve in direction to each other under effect of F_{12} and F_{21} forces, as schematically shown on the Figure.

It is also known [2–6] that curving of the welding arcs provokes so called restorative forces F_1^* and F_2^* preventing indicated curving. At relatively small deviations of arcs ξ_1 and ξ_2 from axial lines of their electrodes, the restorative forces are normal to the deviations, i.e.

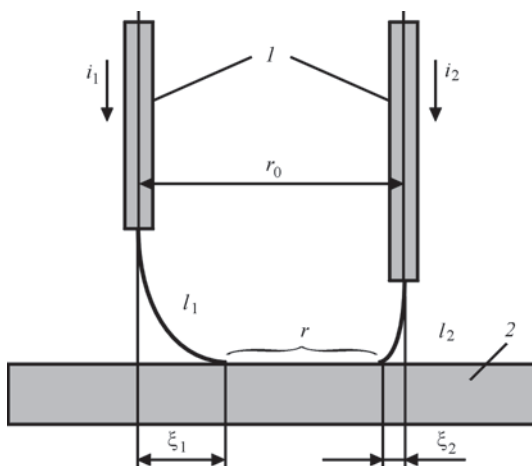
$$F_1^* = -G_1 \xi_1, \quad F_2^* = -G_2 \xi_2. \quad (2)$$

In the expressions (2) G_1 and G_2 are positive coefficients, titled in work [3] as arc rigidity coefficients; they are related with currents i_1, i_2 and arc lengths l_1, l_2 by relationships

$$G_1 = N \frac{i_1^2}{l_1}, \quad G_2 = N \frac{i_2^2}{l_2}, \quad (3)$$

where $N = \text{const}$ is the coefficient depending mainly on welding conditions.

The following important problems appear, namely how big is effect of own magnetic fields on electric arcs in tandem-arc welding with consumable electrode and what are the limitations necessary to be applied to welding currents i_1, i_2 in order to prevent



Scheme of magnetic interaction of two arcs: 1 — consumable electrodes; 2 — part being welded

possible deviations ξ_1 and ξ_2 disturbing stable welding mode?

Based on known publications, these questions are without clear answer up to the moment. Mathematical modelling of electromagnetic interaction of two arcs used for casting of metals and alloys in electric furnaces was carried out in work [7]. The results of modelling are presented in form of non-linear integral-differential equations, which are not very convenient for practical application. Simple relationships between deviations ξ_1, ξ_2 , welding currents i_1, i_2 and lengths of arc gaps l_{10}, l_{20} were received in the paper of Japanese researches [8]. However, these relationships are not very suitable in the case of consumable electrode welding, which, as it is known, have own peculiarities.

An attempt to get answers to the questions mentioned above is made in the present work. At once it should be noted that action of electromagnetic forces on arcs appear not only in the phenomena of microscopic nature, to which change of shape, dimensions and position of arcs in space are referred. Action of electromagnetic fields inside the arcs provokes appearance of Lorentz force, giving centripetal acceleration to charged particles and resulting in spiral movement of these particles. Obviously that indicated forces as well as other nature forces effect arcs spatial position to significantly less degree than F_{12}, F_{21}, F_1^* and F_2^* forces and they are not taken into account in this problem.

For mathematical description of action of F_{12}, F_{21}, F_1^* and F_2^* forces on welding arcs in tandem-arc welding the following idealization is taken:

- arc column, as in works [2, 3], will be considered as flexible thin current conductor, one end of which is «fixed» close to electrode end and another one, located close to weld pool, is «free», i.e. can move along the weld pool;

- forces F_{12}, F_{21}, F_1^* and F_2^* are collinear and normal to axial electrode lines.

Let's write a balance equation of forces acting on «free» ends of welding arcs in scopes of accepted model

$$F_{21} + F_1^* = 0, \quad F_{12} + F_2^* = 0.$$

Taking into account relationship (1)–(3) these equations will become

$$Pl_1 \frac{i_1 i_2}{r} - N \frac{i_1^2}{l_1} \xi_1 = 0, \quad Pl_2 \frac{i_1 i_2}{r} - N \frac{i_2^2}{l_2} \xi_2 = 0,$$

where $P = \mu_0 \mu / (2\pi)$.

Let's re-write the equations in the following way:

$$\xi_1 = \lambda \delta \frac{l_1^2}{r}, \quad \xi_2 = \frac{\lambda}{\delta} \frac{l_2^2}{r}, \quad (4)$$

here $\lambda = P/N$, $\delta = i_2/i_1$ are the dimensionless parameters.

Summing equations (4), we will get

$$\xi_1 + \xi_2 = \frac{\lambda}{r} \left(l_1^2 \delta + \frac{l_2^2}{\delta} \right). \quad (5)$$

On the other hand, it follows that

$$\xi_1 + \xi_2 = r_0 - r, \quad (6)$$

where $r_0 = \text{const}$ is the distance between axial lines of the electrodes.

Equating the right parts of the equations (5) and (6), we will get a quadric equalities relatively to distance between the arc ends r :

$$r^2 - r_0 r + a = 0.$$

A free element of this equation

$$a = \lambda \left(l_1^2 \delta + \frac{l_2^2}{\delta} \right) = \text{const}, \quad (7)$$

and its roots equal

$$r_* = \frac{r_0}{2} + \sqrt{\frac{r_0^2}{4} - a}, \quad r_{**} = \frac{r_0}{2} - \sqrt{\frac{r_0^2}{4} - a}. \quad (8)$$

The roots (8) are real if the condition is fulfilled

$$a \leq \frac{r_0^2}{4}. \quad (9)$$

Obviously that physical meaning has only root r_* (increase of distance r_0 rises r_* distance).

If condition (9) is written in expanded form

$$\delta^2 - \frac{r_0^2}{4\lambda l_1^2} \delta + \frac{l_2^2}{l_1^2} \leq 0, \quad (10)$$

then solution of inequality (10) determine area of allowable values of δ relationship:

$$\delta_m \leq \delta \leq \delta_M, \quad (11)$$

where

$$\delta_m = \frac{r_0^2}{8\lambda l_1^2} - \sqrt{\left(\frac{r_0^2}{8\lambda l_1^2} \right)^2 - \frac{l_2^2}{l_1^2}},$$

$$\delta_M = \frac{r_0^2}{8\lambda l_1^2} + \sqrt{\left(\frac{r_0^2}{8\lambda l_1^2} \right)^2 - \frac{l_2^2}{l_1^2}}.$$

Let's come back to expressions (4) and insert r_* value found in (8) instead of variable r . As a result new desired estimations ξ_1 and ξ_2 are received.

$$\xi_1 = \lambda \delta \frac{l_1^2}{r_*}, \quad \xi_2 = \frac{\lambda}{\delta} \frac{l_2^2}{r_*}. \quad (12)$$

Estimations (12) have approximate nature since parameter λ , rather coefficient N , included in $\lambda = P/N$ relationship is not known exactly and can be determined only in experimental way. Paper [3] provides approximate value $N \approx 5.6\mu_0\mu/(4\pi)$ (in our designations) received as a result of experimental investigation, in which arc rigidity G was determined on measurements of deviations of arc «free» end ξ on axial

line of the electrode under effect on the arc of specially developed transverse magnetic field.

If this result is used, then parameter λ will get the following numerical value:

$$\lambda = \frac{P}{N} = \frac{\mu_0 \mu 4\pi}{2\pi 5.6\mu_0 \mu} \approx 0.35,$$

and desired estimations (12) will take on form of calculation formulae

$$\xi_1 = 0.35\delta \frac{l_1^2}{r_*}, \quad \xi_2 = \frac{0.35}{\delta} \frac{l_2^2}{r_*}. \quad (13)$$

Comparing formulae (13) with formulae

$$\xi_1 = 0.58 \frac{l_{10}^2}{r_0}, \quad \xi_2 = \frac{0.5}{\delta} \frac{l_{20}^2}{r_0}, \quad (14)$$

received in work [8] in a more complex way, we can see that they are similar on shape, but differ in parameters included in them. First of all, arc lengths l_1 and l_2 appearing in formulae (13) in consumable electrode welding do not equal the initial values l_{10} and l_{20} and depend on welding currents in the next way [9]:

$$l_1 = \frac{u_x - u_0}{E} - T v_{e1}, \quad l_2 = \frac{u_x - u_0}{E} - T v_{e2}. \quad (15)$$

In these expressions u_x is the open circuit voltage of welding current sources; u_0 is the sum of near-electrode voltage drops; E is the electric field intensity in welding arcs; v_{e1} and v_{e2} are the rates of feed of the first and second electrodes, respectively; $T = R/(EM)$, where R is the resistance of welding circuits, M is the parameter characterizing electric, thermal-physical and geometry properties of consumable electrodes (it is assumed that both welding circuits are identical).

Secondly, formulae (13) in contrast to (14) contain no distance between the electrodes $r_0 = \text{const}$, but distance between arc ends r_* , which according to expressions (8) and (7) depends on arc lengths l_1 and l_2 , and on relationship between welding currents δ .

Work [8, Figure 3] shows the diagrams representing arc shapes, received as a result of modelling of arc end deviations from axial lines of the own electrodes under the next parameters: $i_1 = i_2 = 9 \cdot 10^3$ A, ($\delta = 1$), $r_0 = 800$ mm, $l_1 = l_2 = 400$ mm. It follows from a diagram, plotted for the case when the arc shapes are approximated by polynomial of the second degree, that at indicated parameters

$$\xi_1 = \xi_2 \approx 80 \text{ mm}. \quad (16)$$

Now let's make calculation of deviations ξ_1 and ξ_2 on formula (13). For this at the beginning on formula (7) find parameter $a = 11.2 \cdot 10^4$ mm². The condition is fulfilled. Then using formula (8) calculate $r_* = 619$ mm and by formulae (13) the next is received

$$\xi_1 = \xi_2 = 0.35 \frac{(400 \text{ mm})^2}{619 \text{ mm}} \approx 90 \text{ mm}. \quad (17)$$

Comparison of estimations (16) and (17) allows concluding that their numerical values are sufficiently close, however, the estimations themselves are received using different methods. It should only be noted that no complex calculation procedures and graphical plotting necessary in order to get the estimation (17).

Efficiency of received results is shown by the example of robotic gas-shielded tandem-arc welding using consumable electrode, performed at the next values of parameters: $u_x = 30$ V, $u_0 = 16$ V, $E = 2$ V/mm, $M = 0.37$ mm/(s·A), $R = 0.04$ Ohm, $r_0 = 10$ mm, $H = 17$ mm (H is the distance between torch edge and part being welded).

Let's consider separately three cases.

1. Rates of electrode feeding v_{e1} and v_{e2} are small. Let's $v_{e1} = v_{e2} = 35$ mm/s. In this case $i_1 = i_2 = v_{e1}/M = 35/0.37 = 95$ A, ($\delta = 1$). Using formula (15) find $l_1 = l_2 = 5.1$ mm and on formula (7) calculate $a = 18.2$ mm². According to (9) $a \leq r_0^2/4 = 25$ mm² condition shall be fulfilled. The condition is fulfilled. Further on formula (8) determine the distance between arc ends $r_* = 7.6$ mm and on formulae (13) calculate deviations

$$\xi_1 = \xi_2 = 0.35 \frac{(5.1 \text{ mm})^2}{7.6 \text{ mm}} = 1.2 \text{ mm}.$$

2. Increase the rates v_{e1} and v_{e2} . Let's $v_{e1} = v_{e2} = 80$ mm/s. Then $i_1 = i_2 = 216$ A, ($\delta = 1$), $l_1 = l_2 = 2.7$ mm, $a = 5.1$ mm², $r_* = 9.5$ mm. Respectively,

$$\xi_1 = \xi_2 = 0.35 \frac{(2.7 \text{ mm})^2}{9.5 \text{ mm}} = 0.3 \text{ mm}.$$

3. Now we consider the case when v_{e1} and v_{e2} rates are different. Let's $v_{e1} = 35$ mm/s and $v_{e2} = 80$ mm/s. In this case $i_1 = 95$ A, $i_2 = 216$ A, ($\delta = 2.3$), $l_1 = 5.1$ mm, $l_2 = 2.7$ mm, $a = 22.0$ mm², $r_* = 6.7$ mm. On formulae (13), find

$$\xi_1 = 0.35 \cdot 2.3 \frac{(5.1 \text{ mm})^2}{6.7 \text{ mm}} = 3.1 \text{ mm},$$

$$\xi_2 = \frac{0.35}{2.3} \frac{(2.7 \text{ mm})^2}{6.7 \text{ mm}} = 0.2 \text{ mm}.$$

Analysis of received results allows making several important conclusions, which, in general, are not obvious.

Conclusions

1. If welding currents of both arcs are equal then they decrease, not rise with increase of arc deviation currents ξ as it may seem from the first sight. This fact in a physical way is explained by the phenomenon that increase of welding currents (by means of rise of feed rate of consumable electrodes v_e at $H = \text{const}$) results in reduction of arc lengths. At that attractive forces F_{12} and F_{21} normal to arc lengths reduce and restor-

ative forces F_1^* and F_2^* reciprocally proportional to arc lengths rise. As a result the points characterizing position of arc ends in relation to axial lines of the own electrodes, are shifted to the side of axial lines, reducing thus arc deviations ξ from indicated lines.

2. If welding currents are different then deviation ξ will be larger in the arc with lower welding current. It is also caused by the fact that arc with lower current has larger length. Therefore, attractive force, acting on longer arc, exceeds attractive force acting on shorter one. Besides, rigidity of longer arc, and, respectively, its restorative force are significantly lower than rigidity and restorative force of shorter arc.

3. Arc deviations ξ significantly depend on relationship between welding currents δ , moreover rise of δ , as can be seen from expressions (12), promotes rapid increase of deviation ξ of longer arc and decrease of that in shorter one. It follows from this that relationship δ can not be taken randomly; it shall be taken in accordance with limitation (11). This is a moment important for practice.

In the conclusion it should be noted that estimations of arc deviations (12) under effect of own magnetic fields were received by us, based on simplified mathematical model, describing these actions. Nevertheless, their comparison with the results given in works [7, 8] brings out clearly that estimations (12) sufficiently well discover functional dependencies be-

tween arc deviations, their lengths, welding currents and distance between the arcs and more convenient for practical application. The necessity in such simple estimations has already appeared at a stage of development of special welding equipment (in particular, welding torch with two isolated electrodes) and the technologies of automated tandem-arc welding using consumable electrode.

1. Dilthey, U., Stein, L., Woeste, K. et al. (2003) Latest developments and trends in high-efficient welding technologies. *The Paton Welding J.*, **10–11**, 146–152.
2. Tikhodeev, G.M. (1961) *Energy properties of welding electric arc*. Moscow-Leningrad, AN SSSR [in Russian].
3. Bachelis, I.A. (1963) On calculation of welding arc deviation in constant transverse magnetic field. *Svarochn. Proizvodstvo*, **7**, 8–11 [in Russian].
4. Kovalev, I.M. (1965) Welding arc deviation in constant transverse magnetic field. *Ibid.*, **10**, 4–6 [in Russian].
5. Leskov, G.I. (1970) *Welding electric arc*. Moscow, Mashinostroenie [in Russian].
6. Lenivkin, V.A. et al. (1989) *Technological properties of welding arc in shielding gases*. Moscow, Mashinostroenie [in Russian].
7. Yachikov, I.M., Kostilyova, E.M. (2014) Mathematical modeling of arcs shape in their electromagnetic interaction. *Izv. Vuzov. Chyorn. Metallurgiya*, **1**, 59–64 [in Russian].
8. Ueyama, T., Ohnawa, T., Yamazaki, K. et al. (2005) High-speed welding of steel sheets by the tandem pulsed gas metal arc welding system. *Transact. of JWRI*, **34**(1), 11–18.
9. Tsybulkin, G.A. (2014) *Adaptive control in arc welding*. Kiev, Stal [in Russian].

Received 15.06.2018

FATIGUE RESISTANCE OF STEEL WELDED JOINTS OF DIFFERENT STRENGTH WITH STEADY RESIDUAL STRESSES

V.A. DEGTYAREV

G.S. Pisarenko Institute for Problems of Strength of the NAS of Ukraine
2 Timiryazevskaya Str., 01014, Kyiv, Ukraine. E-mail: ips@ipp.kiev.ua

A work proposes a comparative analysis of the diagrams of cycle limiting stresses in welded joints of low-carbon and low-alloy steels of different strength under condition that they have the same level of steady residual stresses. By the example of testing of St3sp (killed), 09G2S and 14KhMNDFR steel butt welded joints it is shown that the welded joints with larger mechanical properties have higher endurance limits in all investigated range of change of the limiting steady residual stresses. It was found that the welded joints of stronger steels have also higher values of endurance limit at the same relative value of cycle average stress. They rise more intensively with increase of the relative values of cycle average stress. 10 Ref., 2 Tables, 5 Figures.

Keywords: *welded joint, cycle stress amplitude, cycle average stress, yield limit, steady residual stress, endurance limit, diagram of cycle limiting stresses*

Investigations carried in work [1] have determined that the diagrams of cycle limiting stresses (DCLS) of butt welded joints from low-carbon and low-alloy steels of different strength with high residual tension stresses (RS) in the field of limited life (to number of load cycles $N = 5 \cdot 10^5$) diverge with rise of a coefficient of cycle asymmetry R_σ , that shows advantage of higher strength steels. At that, they have similar endurance limit at symmetric stress cycle. DCLS of welded joint of different strength steels match at $N > 2 \cdot 10^6$ starting from symmetric cycle and up to specific positive value R_σ . This means that the diagram of stronger joints is continuation of one reflecting fatigue resistance of less strong joint. The results of investigations of other types of welded joints showed the same behavior of the diagrams of cycle limiting stress at $N > 2 \cdot 10^6$ [2]. Presentation of the investigation results in form of combined diagrams allowed determining the areas of reasonable application of steels of different strength in the elements of metal structures with non-processed welded joints that, undoubtedly, have large practical value. Analysis of publications carried in work [3] showed that each point on DCLS at different cycle average stresses σ_m or R_σ corresponds to endurance limit of welded joint with own value of limiting steady residual stress σ_{res}^s . Since it is well known [4] that initial residual stresses rise in proportion to yield limit of base material σ_y then their values are larger in welded joints of higher strength steels. Therefore, regardless similar received values of the endurance limits on matching section of the diagrams, i.e. at similar

stresses from external load, welded joints of higher strength steels will have larger final RS. And taking into account that σ_{res}^s value at other conditions being equal plays an important role in reduction of fatigue resistance, the test results of the welded joints containing different level of σ_{res}^s are compared. Besides, it should be noted that the similar endurance limits for welded joints of different strength are received at different relationship of average stress to material yield limit, i.e. at different relative value of cycle average stress.

In this connection it is interesting to carry out the investigations which allow matching fatigue resistance of welded joints of different strength class steels containing similar level of limiting final RS and the same relative value of cycle average stress in R_σ range of changing, at which matching of the diagrams of cycle limiting stresses takes place.

Analysis of received results. The analysis carried out on the example of testing the butt welded joints of low-carbon steel St3sp (killed) ($\sigma_y = 300$ MPa), low-alloy steel 09G2S ($\sigma_y = 340$ MPa) and low-alloy high-strength steel 14KhMNDFR ($\sigma_y = 600$ MPa). The maximum initial tension RS according to work [4] depending on steel strength class are in the range of (0.75–0.85) σ_y , i.e. on average make 260, 290 and 450 MPa in the welded joints of St3sp (killed), 09G2S and 14KhMNDFR steels, respectively. Figure 1 shows the results of fatigue tests of butt welded joints with RS of low-carbon and low-alloy steels with different strength [4] in form of the combined diagrams of cycle limiting stresses. It can be seen that their endur-

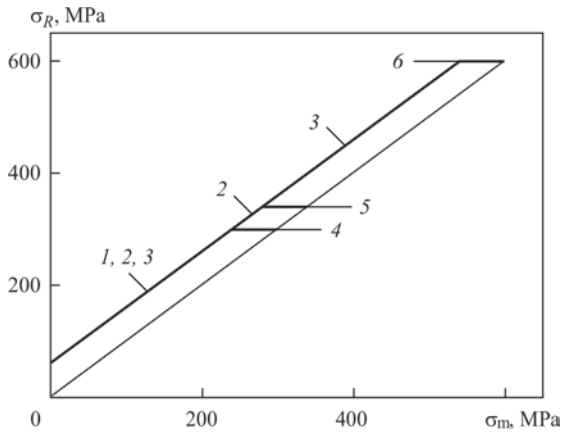


Figure 1. Diagrams of cycle limiting stresses in butt welded joints with RS of low-carbon (1), low-alloy (2) and low-alloy high-strength (3) steels, 4-6 — material yield limits

ance limits σ_R match in the range of R_σ changing from -1 to 0.6 or average cycle stress σ_m to 235 MPa. Since the stress limiting amplitude σ_a does not depend on σ_m , the diagrams of cycle limiting stresses of welded joints can be described in form of dependence

$$\sigma_R = \frac{2\sigma_{-1}}{1 - R_\sigma}, \quad (1)$$

where $\sigma_{-1} = 65$ MPa is the endurance limit of welded joint with RS at symmetric cycle of loading.

In present work an effect of theoretical coefficient of stress concentration was not considered by the reason of accepted in the references [5-7] determination of DCLS or diagrams of cycle limiting amplitudes (DCLA) only due to effect of nominal stresses. The effect of RS and stresses, caused by static loading, were supposed to be identical [8]. It also follows from the Figure analysis that the values of final RS as well as relationship of limiting stresses to material yield limit will be different at similar values of endurance limits in the welded joints of steels with various strength.

It is known that increase of average cycle stress under condition of reaching the maximum stresses (taking into account residual ones) of material yield limit provokes reduction of initial RS till the final level. The investigations [3] carried before allowed determining DCLS or DCLA of the joints with different value of σ_{res}^s using the results of tests of the welded joints without RS defined on formulae:

$$\sigma_R = \sigma_{-1m} + (1 - \psi_\sigma)\sigma_m - \psi_\sigma \cdot \sigma_{res}^s, \quad (2)$$

Table 1. Calculation limiting stresses (MPa) for different level of final RS in welded joints of steels St3sp and 14KhMNDFR

Steel	σ_{res}^s , MPa											
	0		50		100		200		300		400	
	σ_R	σ_m	σ_R	σ_m	σ_R	σ_m	σ_R	σ_m	σ_R	σ_m	σ_R	σ_m
St3sp ($\sigma_{-1m} = 108$ MPa, $\psi_\sigma = 0.183$)	300	235	250	185	200	135	100	35	—	—	—	—
14KhMNDFR ($\sigma_{-1m} = 110$ MPa, $\psi_\sigma = 0.085$)	600	535	—	—	500	435	400	335	300	235	200	135

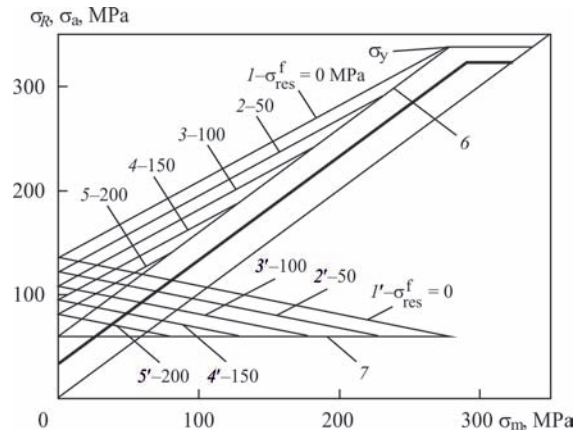


Figure 2. Diagrams of limiting stresses (1-5) and cycle limiting amplitudes (1'-5') of butt welded joints of low-alloy steel 09G2S: 1, 1' — without RS; 2-5, 2'-5' — with steady RS; 6, 7 — lines of limiting stresses and cycle minimum limiting amplitude, respectively

or

$$\sigma_a = \sigma_{-1m} - \psi_\sigma (\sigma_m + \sigma_{res}^s), \quad (3)$$

where σ_{-1m} is the endurance limit of the welded joint without residual stresses; ψ_σ is the coefficient of sensitivity to asymmetry of stress cycle.

Figure 2 shows as an example in general form such diagrams of butt welded joint from steel 09G2S with different level of σ_{res}^s . It can be seen that an inclined section of the diagram is shifted by $\Delta\sigma_a = \psi_\sigma \sigma_{res}^s$ value parallel to the diagrams of welded joints without RS and with rise of σ_{res}^s each further diagram is placed below the previous one. They are ended on lines 6 and 7 where each point on these lines correspond to the cycle limiting stress or cycle minimum limiting amplitude σ_a^l of welded joint with own values of limiting ones σ_{res}^s that provides realizing of the limiting stress cycle. At that the average stress, which in this case is also the limiting one, is shifted by $\Delta\sigma_m = \sigma_{res}^s$ value. Table 1 provides the necessary calculation values of the limiting stresses allowing determining the same diagrams of welded joints of other strength steels at different σ_{res}^f values. Following the limited number of experimental data [9] as well as reference data, given in work [10], it can be assumed that DCLS of 14KhMNDFR steel welded joints without RS can have parabolic nature. In this case ψ_σ will be variable value. Therefore, for convenience of calculations the

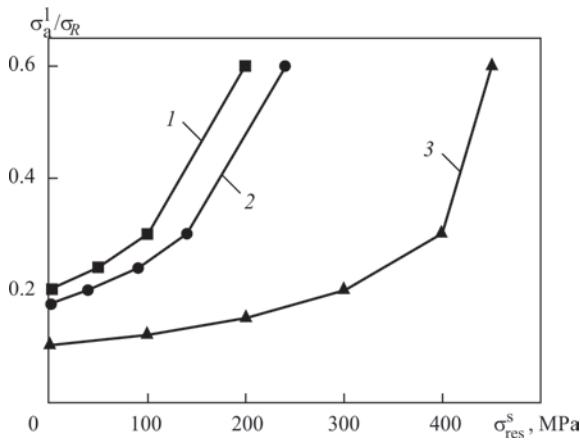


Figure 3. Dependencies between relationship of cycle minimum limiting amplitude to endurance limit and limiting steady RS in butt welded joints of steels St3sp (1), 09G2S (2) and 14KhMNDFR (3)

diagram was somewhat idealized and presented in form of a line.

Presentation of data in such a form allows coming to determination of cycle limiting stresses of the welded joints from researched steels at similar level of final RS. Sensitivity of the butt welded joints to σ_{res}^s value is shown in Figure 3. Taking into account experimental and calculation data, the Figure shows the dependencies between a relationship of stress limiting amplitude to corresponding endurance limit and value of final RS. In this case the most interesting characteristic, i.e. the cycle minimum limiting amplitude was considered. At that the single limiting stress cycle is realized. The analysis of received results shows that the similar values of σ_{res}^s in the welded joints of steels with higher mechanical properties are reached at lower σ_a^l/σ_R . And this difference rises with increase of σ_{res}^s . Also, it is not difficult to determine σ_{res}^s value at the same σ_a^l/σ_R relationship. For example, $\sigma_a^l/\sigma_R = 0.5$ in the welded joints of St3sp and 14KhMNDFR steels can be received at σ_{res}^s being equal 170 and 440 MPa, respectively. Using received data Figure 4 represents the dependencies of endurance limits of

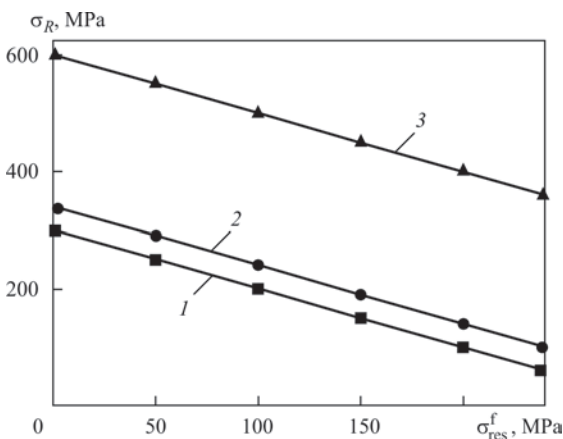


Figure 4. Dependencies of endurance limits of butt welded joints of St3sp (1), 09G2S (2) and 14KhMNDFR (3) steels on limiting steady RS

the welded joints from the investigated steels on limiting final RS under condition that different strength welded joints, as it was mentioned above, have similar endurance limit at symmetric cycle or similar minimum limiting amplitude of stresses on external load, that is the same, equal to 65 MPa. The analysis of presented results showed that rise of σ_{res}^s provokes reduction of endurance limits of welded joints from low-carbon and low-alloy steels of different strength. However, they remain increased in all investigated range of σ_{res}^s changing in welded joints with higher mechanical properties. For example, at change of σ_{res}^s from 50 to 200 MPa, σ_R of welded joint of low-alloy high-strength steel is higher 2.2 and 4.0 times, respectively, in comparison with low-carbon steel. If at σ_{res}^s equal to 200 MPa the endurance limit of low-carbon steel welded joint decreases 3 times than that for welded joint of high-strength steel is only 1.5 times. Thus, received results indicate the rise of endurance limits of welded joints with increase of strength of steels in investigated range of measurement of limiting steady RS.

Besides, if DCLS of welded joints shown in Figure 1 are presented in relative coordinates (Figure 5) it can be seen that they initially diverge at similar relative values of average stresses from external loading σ_m/σ_y . At that, welded joints of higher strength steels have larger relative values of the endurance limit, varying inclination angle of the diagram to larger extent. Presentation of data in such a form allows considering mechanical properties of researched steels, analyze obtained results in comparable test conditions. In general terms the equation for each line can be written as

$$\frac{\sigma_{Ri}}{\sigma_{-1}} = 1 + K \left(\frac{\sigma_m}{\sigma_y} \right), \quad (4)$$

where $K = \sigma_{yi}/\sigma_{-1}$ is the angle of line inclination; σ_{yi} is the yield limit of the material of corresponding steel.

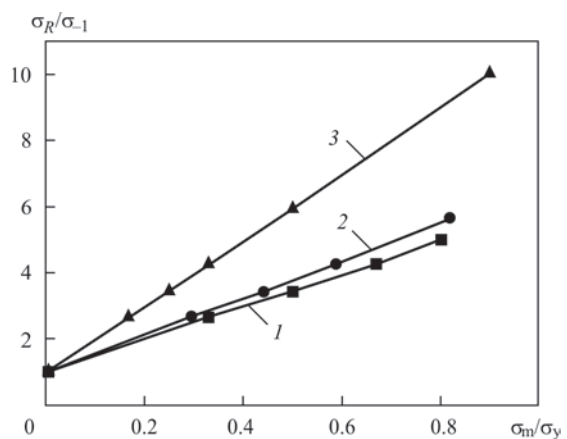


Figure 5. Dependencies between relative values of endurance limits of butt welded joints from St3sp (1), 09G2S (2) and 14KhMNDFR (3) steels and cycle average stresses

This provides the possibility for determination of DCLS of welded joints of investigated steels, knowing the equation for one of them. It is enough to write down an equation of diagram of cycle limiting stresses, for example, of welded joint of St3sp steel (line 1) in form of

$$\frac{\sigma_{Rl}}{\sigma_{-1}} = 1 + \frac{\sigma_{yl}}{\sigma_{-1}} \left(\frac{\sigma_m}{\sigma_y} \right) \quad (5)$$

and solving it relatively to σ_m/σ_y , determine DCLS equation for welded joint of other strength steel, which will be in a form

$$\sigma_{Rl} = \sigma_{-1} + \frac{\sigma_{yl}}{\sigma_{-1}} (\sigma_{Rl} - \sigma_{-1}). \quad (6)$$

As an example Table 2 gives, following formulae (5) and (6), the calculation values of endurance limits of welded joints from investigated steels at different values of σ_m/σ_y . The analysis of table data showed that the endurance limit of steel rises with increase of steel strength at similar relationship of σ_m/σ_y , i.e. in testing under comparable conditions. Moreover, increase of this relationship rises the difference between the endurance limits.

Using the data, given in Figures 4 and 5, it is possible to determine the values of cycle average stress, at which similar final RS and vice versa act in the welded joints of investigated steels. For example σ_m in the welded joints of St3sp, 09G2S and 14KhMNDRF steels equal 85, 120 and 380 MPa, respectively, at $\sigma_{res}^s = 150$ MPa. In turn, at $\sigma_m/\sigma_y = 0.5 \sigma_{res}^s$ values in the welded joints make to 85, 100 and 230 MPa with improvement of mechanical properties of material. This corresponds to 0.28–0.38 of yield limit of corresponding steel. Besides, in the absence of full-scale investigations it is also not difficult to determine DCLS of the investigated welded joints. For this by means of combined solution of dependencies (2) and (4) for set value σ_m it is enough to determine the value of steady RS as

$$\sigma_{res}^s = \frac{\sigma_{-1m} - \sigma_{-1} - \psi_\sigma \sigma_m}{\psi_\sigma}, \quad (7)$$

and then using formula 2 the endurance limits of welded joints of investigated steels with available σ_{res}^s are determined.

Thus, received data allowed comparing the limiting stresses in welded joints of different strength steels at similar level of steady RS as well as relatively to acting stresses from external loading that can help in steel selection for known operation conditions.

Table 2. Endurance limits of welded joints from investigated steels

Steel	Endurance limits σ_R , MPa at different σ_m/σ_y				
	0	0.1	0.3	0.5	0.7
St3sp (killed)	65	95	155	215	275
09G2S	65	100	167	235	305
14KhMNDRF	65	125	245	365	485

Conclusions

1. The procedure was proposed for determination of diagrams of the cycle limiting stresses in butt welded joints of different strength class. It allows determining dependencies of change of endurance limits of welded joints at similar level of limiting steady residual stresses and relative stresses from external loading.

2. It is determined that the welded joints of stronger steels have larger steady residual stresses and higher values of endurance limit at similar relative value of cycle average stress. Increase of relative values of cycle average stresses promotes more intensive rise of endurance limits of the welded joints from stronger steels.

3. Increase of endurance limits of the welded joints with rise of steel strength in the investigated range of changes of limiting steady residual stresses is shown.

1. Knysh, V.V. Solovej, S.A. (2017) *Improvement of service life of welded joints with fatigue damages*. Kiev, KPI [in Russian].
2. (2014) *Steel structures*. Design standards DBN V.2.6-198 [in Russian].
3. Degtyarev, V.A. (2016) Prediction of limiting amplitudes of cycle stresses of welded joints with steady residual stresses. *The Paton Welding J.*, **10**, 14–19.
4. Trufyakov, V.I. (1973) *Fatigue of welded joints*. Kiev, Naukova Dumka [in Russian].
5. Troshchenko, V.T., Tsybanov, G.V., Gryaznov, B.A., Nalimov, Yu.S. (2009) *Strength of materials and structures. Fatigue of metals. Influence of surface state and contact interaction*. Kiev, IPS, Vol. 2 [in Russian].
6. Krizhanovsky, V.I., Kasperskaya, V.V., Pogrebnyak, A.D. (2008) Evaluation of limit state of structural steels under asymmetric multicycle loading by tension, compression, bending and torsion. *Problemy Prochnosti*, **5**, 81–88 [in Russian].
7. Golub, V.P. (2001) Experimental analysis of high-temperature creep, fatigue and damage. 1: Analysis methods. *Int. Appl. Mech.*, **37**, 4, 425–455.
8. Pavlov, V.F., Kirpichyov, V.A., Ivanov, V.B. (2008) *Residual stresses and fatigue resistance of strengthened parts with stress concentrators*. Samara, OOO Izd-vo SNTs [in Russian].
9. Myunze, V.Kh. (1968) *Fatigue strength of welded steel structures*. Moscow, Mashinostroenie [in Russian].
10. Oding, I.L. (1962) *Acceptable stresses in machine-building and cyclic strength of metals*. Moscow, Mashgiz [in Russian].

Received 23. 01.2018

INFLUENCE OF RARE-EARTH ELEMENTS ON THE STRUCTURE AND PROPERTIES OF WELDS OF VT22 TITANIUM ALLOY

S.L. SCHWAB, I.K. PETRYCHENKO and S.V. AKHONIN

E.O. Paton Electric Welding Institute of the NAS of Ukraine
11 Kazimir Malevich Str., 03150, Kyiv, Ukraine. E-mail: office@paton.kiev.ua

The paper presents the results of investigations of the influence of rare-earth metal fluorides on structural changes in weld metal of titanium alloy VT22 for the purpose of using them in the flux filler of experimental flux-cored wire for welding this alloy. It was shown that refinement of β -grains is observed in welds made by argon-arc welding of VT22 alloy over a layer of flux, consisting of rare-earth metal fluorides. Addition of LaF_3 to the core of experimental flux-cored titanium wire PPT-22 in combination with heat treatment allowed increasing the impact toughness of welds in argon-arc welding of VT22 alloy 2 times up to 30.6 J/cm^2 . 8 Ref., 4 Tables, 5 Figures.

Keywords: VT22 titanium alloy, rare-earth metal, fluorides, flux-cored wire

Argon-arc welding (AAW) is the most versatile method of joining structures from titanium components, as it allows performing welding in different positions, quickly readjusting the equipment at the change of the joint type and thickness of metal being welded [1, 2]. In view of the high chemical activity, titanium at increased temperatures and particularly in the molten state actively absorbs oxygen and nitrogen, leading to abrupt lowering of ductility. Therefore, welded joint quality is determined, mainly, by reliability of welding zone shielding, and the main difficulty of titanium welding is ensuring reliable shielding from the atmosphere not only of the weld pool and weld root, but also of the cooling areas of welded joint heated above $400 \text{ }^\circ\text{C}$, i.e. up to temperatures, at which a noticeable interaction of titanium with gases, namely oxygen, hydrogen and nitrogen, begins.

One of the advantages of welding titanium with flux application is presence of molten flux skin covering the welding zone and protecting it from harmful influence of O_2 , H_2 and N_2 . During welding, metallurgical reactions are taking place, which may lead to weld enrichment with these impurities. Therefore, one of the requirements to flux systems in titanium welding is absence of oxides in them. It is proved [3] that oxide removal from the fluxes allows limiting oxygen content in the deposited metal below 0.1 %.

Main requirements, made of the flux for titanium welding, are determined, primarily, by comparatively high temperature of titanium melting, so that welding fluxes for it should feature an increased refractoriness [3]. To avoid weld saturation with hydrogen, the flux should have minimum hygroscopicity; provide stabil-

ity of the arc discharge during welding, and after it is over — easy separation of the slag crust from the solidified weld metal, that is one of the criteria of flux system adaptability to fabrication.

From the viewpoint of adaptability to fabrication, none of the fluorides of alkali and alkali-earth elements is suitable as a one-component flux. Therefore, multicomponent systems, consisting of fluorides of alkali, alkali-earth and rare-earth metals, as well as alkali-earth metal chlorides are applied as fluxes in titanium welding [3].

Application of fluoride fluxes at AAW of titanium leads to reduction of weld pool dimensions, shortening of the time of metal being in the molten state, and also binds hydrogen into TiF_xH_y compounds insoluble in the metal, that lowers the probability of initiation of gas phase nuclei in the weld pool and inhibits pore formation in liquid titanium.

An important property of calcium fluoride in the flux system is its ability to intensively interact with water vapour with formation of hydrogen fluoride. Possibility of removing moisture from the welding zone and, due to that, protection of weld metal from saturation with hydrogen and oxygen, is an important feature of titanium welding using CaF_2 -based flux. Therefore, the authors selected exactly this component as the base of the flux system.

Experimental method also revealed that a characteristic feature of the slag crust is noted in welding with BaF_2 . It easily spalls off in whole pieces from the joint surface. For this purpose, it is necessary to add this component to the flux system.

To improve the refractoriness of the flux system, it is necessary to add a component with higher melting

temperature (Table 1). It is known [4] that CaF_2 - BaF_2 , CaF_2 - SrF_2 and SrF_2 - BaF_2 systems are a continuous row of solid solutions. Among them, CaF_2 - SrF_2 system has the highest melting point. Therefore, transition from two-component CaF_2 - BaF_2 system to CaF_2 - SrF_2 - BaF_2 system should lead to increased melting temperature of the flux.

Having studied the influence of fluorides of alkali and alkali-earth metals on titanium welding process, the authors selected CaF_2 - SrF_2 - BaF_2 system, which was the flux base in the core of flux-cored wire PPT-22 for VT22 titanium alloy welding. This wire consists of a sheath from VT1 titanium alloy and core (granules of VT22 alloy and flux component) [5].

Reference [3] is a study of the possibility of weld metal refining by adding to flux such elements active to oxygen and nitrogen, as cerium, lanthanum, yttrium in the form of fluorides. The most active refining action is produced by yttrium, the least active is produced by cerium, with lanthanum taking an intermediate position. It is found that not more than 10 % of these fluorides should be added to the flux to refine the weld metal. Then, oxygen content in the weld metal will be equal to 0.09 % and with further increase of LaF_3 or YF_3 content in the flux, it will remain constant.

The authors of [6] studied the possibility of modifying the weld metal using fluxes containing fluorides of rare-earth metals. The work shows that in welding of titanium β -alloy VT15 using flux, containing LaF_3 , refinement of weld structure, improvement of mechanical properties of weld metal and lowering of oxygen content in it are observed. Increase of its ductile properties and impact toughness is noted. Chemical-spectral method showed that metallurgical interaction of liquid metal and molten flux, having LaF_3 in its composition, is accompanied by lanthanum transition into the weld metal.

This work is a study of the influence of rare-earth metal fluorides on structural changes in weld metal of VT22 alloy, in order to use them in the composition of flux filler of flux-cored wire PPT-22.

Features of the influence of rare-earth metal fluorides in welding on structural changes in weld metal of VT22 alloy. Studies were conducted on welded samples 6 mm thick from VT22 alloy, produced by AAW over flux in one pass and without flux application. Experiments were performed with fluorides of LaF_3 and YF_3 rare-earth metals in the following mode: $I_w = 200$ A, $v_w = 8$ m/h; $L_a = 2$ mm, $U_a = 12.5$ – 13.0 V.

Comparison of microstructure of the produced deposits showed that in welding over LaF_3 and YF_3 fluxes the weld shapes do not differ from each other, weld width being 13.5 mm in both the cases. In the

Table 1. Physical properties of flux system components

Component properties	CaF_2	SrF_2	BaF_2
Temperature, °C			
melting	1411	1473	1280
boiling	2500	2460	2260
Density, g/cm ³	3.18	4.18	4.83
Heat of formation, kJ/mole	608	1222	599.1

weld made by AAW without flux, the maximum penetration depth is 2.5 mm and its maximum is on weld axis; and in the case of AAW over LaF_3 and YF_3 fluxes penetration is on the same level and is practically the same across the entire weld width (Figure 1).

In all the three variants after welding the weld metal consists of β -phase grains of different dimensions and shape. Most of β -grains have a non-equiaxial form, grain form factor (length-to-width ratio) is equal to 1–5, grains are elongated in the vertical or close to the vertical direction (Figure 2, *a*, *c*, *e*).

It is known [7] that interaxial and interdendrite spaces in the weld metal are enriched in β -stabilizers to a greater degree than the inner volumes of the axes, so that the most intensive decomposition of β -phase occurs in the inner volumes as the least stable regions. The most intensive decomposition of β -solid solution after welding occurred in the weld made by AAW without flux application (Figure 2, *e*). It is obvious that the conditions of cooling of the metal of welds made with application of fluxes, differ from those in welds made without flux application.

Intensity of β -phase decomposition in welds of VT22 alloy depends on the cooling rate after welding, and the higher the cooling rate, the lower is the intensity of decomposition. For instance, metastable β -phase is found in welds of VT22 alloy made by EBW and characterized by very high cooling rate, whereas a significant decomposition of β -phase proceeds in welds, made by ESW and featuring a much lower cooling rate. After AAW with application of yt-

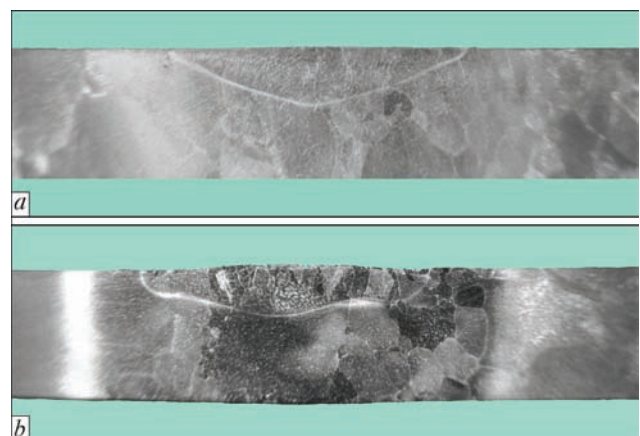


Figure 1. Macrosections of welded joints of VT22 alloy made by AAW: *a* — without flux; *b* — over YF_3 flux

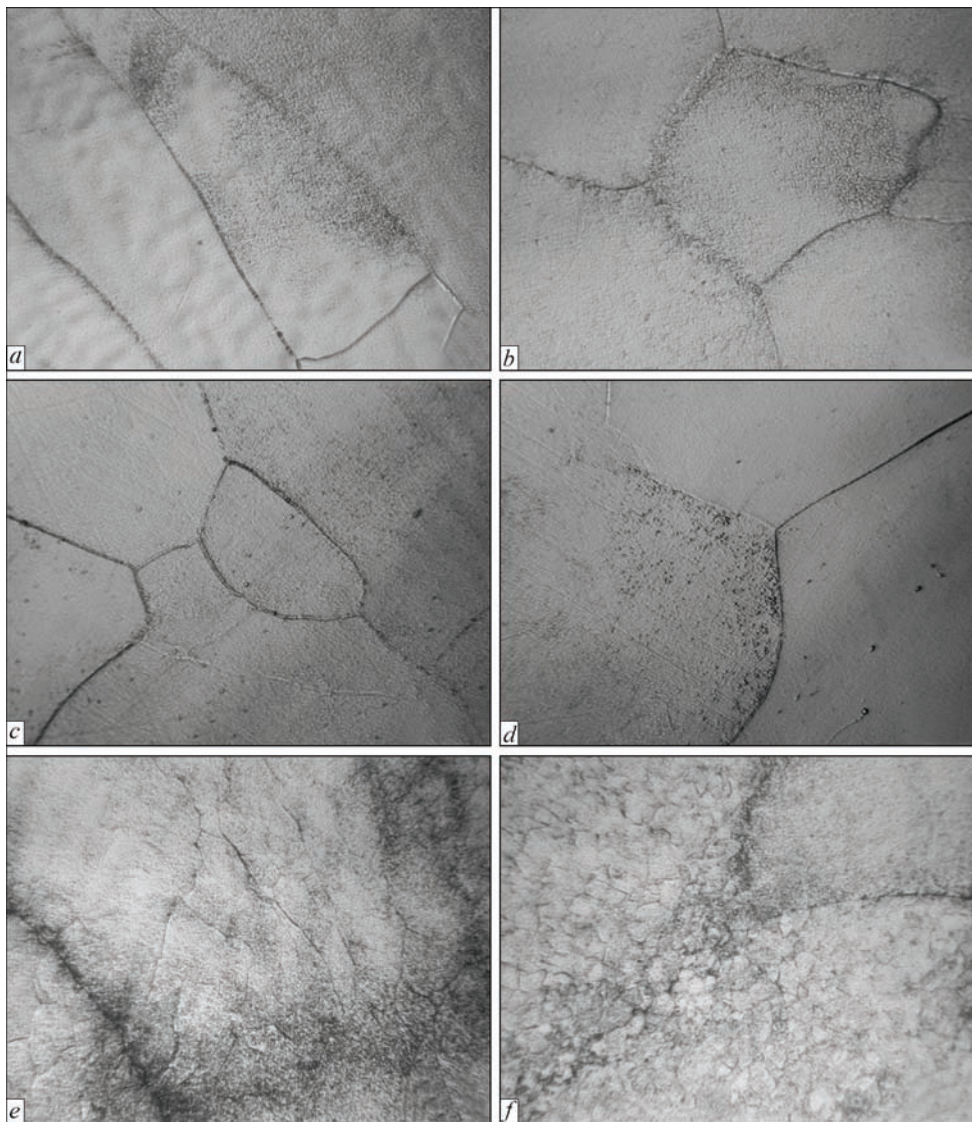


Figure 2. Microstructure ($\times 200$) of welded joints: *a* — weld made by AAW over YF_3 flux; *b* — HAZ of a sample with YF_3 ; *c* — weld made by AAW over LaF_3 flux; *d* — HAZ of a sample with LaF_3 ; *e* — weld made by AAW without flux; *f* — HAZ of a sample without flux

trium and lanthanum fluorides, the intensity of β -solid solution decomposition is lower than after AAW without flux. Structure analysis confirms the known fact that the cooling rate of the metal of weld, made with flux application, is higher.

In addition to difference in the intensity of β -phase decomposition in welds, we can note that polygonization processes are very well developed in the weld lower part, particularly, in the HAZ of the sample welded by AAW without flux. Coarse grains of β -phase after AAW without flux application have a developed substructure (Figure 2, *e, f*), unlike samples welded by AAW over LaF_3 and YF_3 fluxes (Figure 2, *a-d*). Under the action of welding deformations, individual grain fragments in coarse β -grains rotate relative to each other by an angle of several degrees, forming a substructure.

It should be noted that in welds made by AAW over flux consisting of fluoride of a rare-earth metal

(LaF_3 or YF_3), refinement of β -grains is observed in as-welded condition, compared to AAW without flux application. Analysis of grain distribution in welds over their cross-sectional area showed that the microstructure of the metal of a weld made by AAW without flux application, consists of a small number of large β -grains, and in welds, made with application of fluorides of both yttrium and lanthanum, the number of small grains is much higher than in the weld made without flux application. For instance, in the weld, produced with rare-earth metal fluoride, 10 times more grains of up to 0.1 mm^2 area appear, compared to a similar region of the weld, produced without lanthanum or yttrium participation (Figure 3).

Microhardness values (Figure 4) of welds made with LaF_3 and YF_3 are on the level of 3450 MPa that is 150 MPa higher than those of welds made without addition of rare-earth elements and is closer to microhardness values of base metal (3800 MPa).

Table 2. Parameters of sample welding modes

Pass number	I_w, A	U_a, V	$v_w, m/h$	$v_w, m/h$
1	180	10.5	9	24
2, 3	200	12.0	9	30

Table 3. Results of mechanical testing of as-welded joints

Test location	σ_r, MPa	$KCV, J/cm^2$
Base metal	1039.7*	32.6
Welded joint with LaF_3	865.3	8.9
Weld metal without LaF_3 [5]	1065.1	5.9

*The paper gives the results of testing three samples.

Thus, application of rare-earth elements in welding of two-phase ($\alpha + \beta$)-titanium alloy VT22 at weld microhardness values close to those of base metal, leads to refinement of β -grains in the weld, that, in its turn, creates prerequisites for increase of weld ductility. Therefore, the authors of this work studied addition of rare-earth element fluorides to the flux component of flux-cored wire for welding VT22 titanium alloy.

Welding and heat treatment of VT22 alloy with filler wire containing rare-earth elements. Welding was performed on plates from VT22 alloy 8 mm thick, in three passes with 90° edge preparation (Table 2). Welding was conducted with application of an external transverse alternating magnetic field (20 Hz frequency, 4 mT value of magnetic inductance) for moving the arc column and weld pool, respectively, across the weld. Experimental flux-cored wire PPT-22 of 2.9 mm diameter was used as filler material. Flux of $CaF_2-SrF_2-BaF_2-LaF_3$ system was added to the flux filler of the wire.

Results of mechanical testing of welded joint (Table 3) showed that ultimate strength of weld metal with LaF_3 participation is lower than without it. However, impact toughness of welded joint with LaF_3 , is 30 % higher that can be due to fine-grained structure of weld metal. Note that all the tensile samples failed not in the weld, but outside it, in the HAZ.

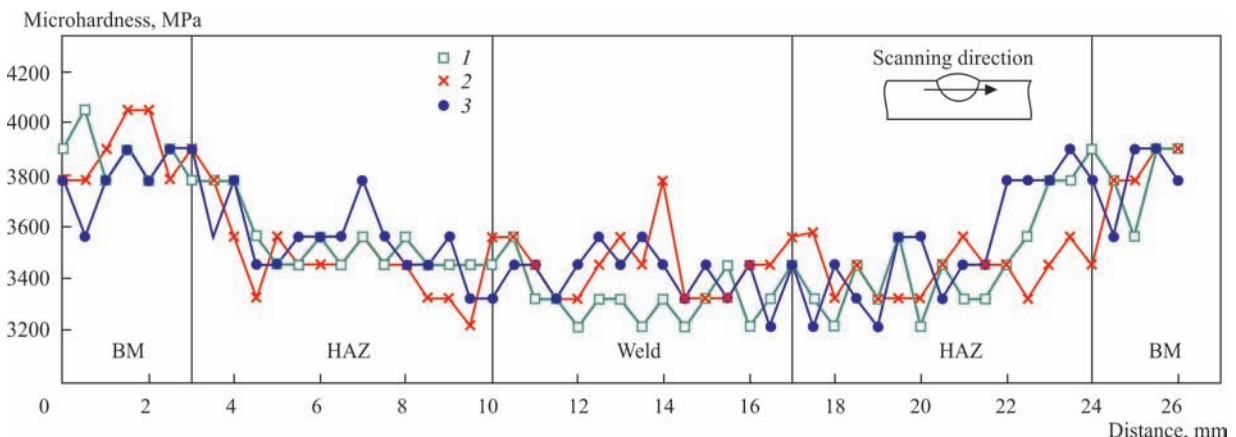


Figure 4. Microhardness of welded joints made by AAW without flux (1), over YF_3 flux (2) and over LaF_3 flux (3)

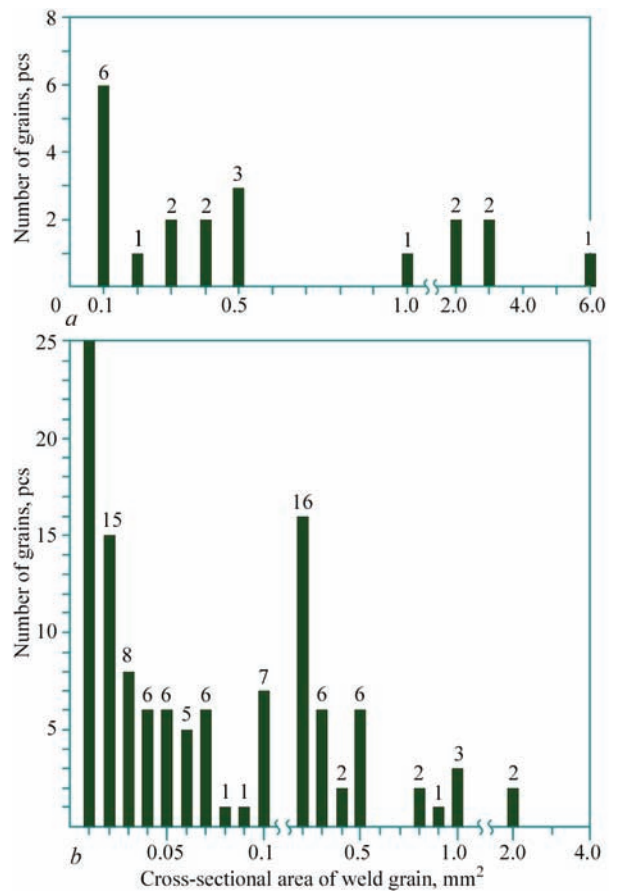


Figure 3. Histograms of distribution of the number of grains in welds of VT22 alloy, depending on their cross-sectional area: a — AAW without flux; b — AAW over YF_3 flux

Welded joints of VT22 titanium alloy are subjected to heat treatment (HT) to improve their mechanical properties. HT of titanium alloys is based mainly on polymorphous $\alpha \leftrightarrow \beta$ transformation. As a result of HT, the structure is stabilized, ductility and impact toughness of welds are considerably increased. At the same time, inner stresses arising during welding become lower.

In VT22 alloy with a significant content of β -phase, not only recrystallization processes occur, but phase composition also changes essentially at HT. This

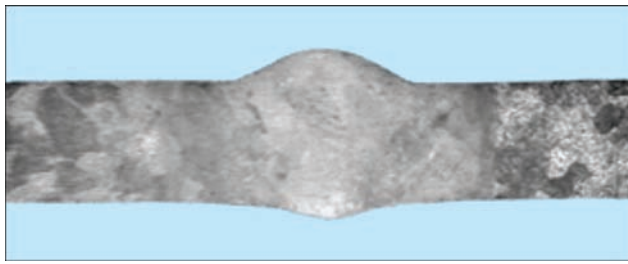


Figure 5. Macrosection of welded joint produced with flux-cored wire PPT-22 after two-step HT

greatly influences the mechanical properties. Changes in phase composition are controlled by cooling rates, as well as different steplike heating cycles.

At selection of HT mode, recrystallization temperature affecting the nature of phase transformations should be taken into account. Proceeding from analysis of published data [7, 8] quite simple technological process was selected for HT of welded joints made with application of flux-cored filler wire: soaking in the furnace at the temperature of 750 °C for 1 h, cooling with the furnace.

Investigation of weld metal macrostructure after annealing showed that annealing promoted formation of a homogeneous and uniform structure of the metal by weld height (Figure 5).

Analysis of obtained results of mechanical testing of samples shows positive summary influence of HT at addition of LaF_3 to the flux filler. As a result, at a slight decrease of strength (by 10 %), compared to samples without addition of rare-earth elements, impact toughness of the joint with LaF_3 is 2 times higher than that without its addition, and 35 % higher than base metal values (Table 4).

Investigation results show that addition of rare-earth elements to the flux component of flux-cored wire for welding VT22 titanium alloy influences the

Table 4. Results of mechanical testing of base metal and welded joint after HT

Test location	σ_t , MPa	KCV, J/cm ²
Base metal	1057.5*	19.6
Welded joint with LaF_3	955.4	30.6
Welded joint without LaF_3 [5]	1121.6	14.8

*The paper gives the results of testing three samples.

structural features of weld formation, namely, increase of the number of fine grains. It is shown that HT of welded joints of VT22 alloy, made by multipass welding with experimental filler wire PPT-22, promoted 2.5 times increase of impact toughness of the joints. Addition of LaF_3 to the wire allowed achieving an increase of impact toughness by 2 more times (up to 30.6 J/cm²) that is higher than base metal values.

- (2003) *Titanium and titanium alloys. Fundamentals and applications*. Ed. by C. Leyens. Germany, Wiley-VCH.
- Inozemtsev, A.A., Bashkatov, I.G., Koryakovtsev, A.S. (2010) *Modern titanium alloys and problems of their development*. Moscow, VIAM [in Russian].
- Gurevich, S.M., Zamkov, V.N., Blashchuk, V.E. et al. (1986) *Metallurgy and technology of welding of titanium and its alloys*. 2nd ed. Kiev, Naukova Dumka [in Russian].
- (1977) *Diagrams of meltability of salt systems*: Refer. book; Pt 1. Ed. by Posypajko, V.I. et al. Moscow, Metallurgiya [in Russian].
- Prilutsky, V.P., Schwab, S.L., Petrychenko, I.K. et al. (2016) Argon arc welding of titanium VT22 alloy using filler flux-cored wire. *The Paton Welding J.*, **9**, 9–13.
- Gurevich, S.M., Zamkov, V.N., Zagrebenyuk, S.D. et al. (1964) Influence of fluxes containing rare-earth elements on structure and properties of welds of VT15 alloy. *Avtomatich. Svarka*, **4**, 93–94 [in Russian].
- Grabin, V.F. (1975) *Basics of physical metallurgy and heat treatment of welded joints from titanium alloys*. Kiev, Naukova Dumka [in Russian].
- Lyasotskaya, V.S. (2003) *Heat treatment of welded joints from titanium alloys*. Moscow, Ekomet [in Russian].

Received 31. 01.2018

ON MECHANISM OF WELD METAL STRUCTURE REFINEMENT IN ARC WELDING UNDER ACTION OF MAGNETIC FIELDS (REVIEW)

A.D. RAZMYSHLYAEV¹ and M.V. AGEEVA²

¹SHEI «Pryazovskyi State Technical University»

7 Universitetskaya Str., 87500, Mariupol, Donetsk region, Ukraine. E-mail: razmyshlajev@rambler.ru

²Donbass State Engineering Academy

72 Akademicheskaya Str., 84313, Kramatorsk, Donetsk region, Ukraine. E-mail: maryna_ah@ukr.net

Aim of the work is the analysis of available references on mechanism of refinement of weld structure in arc welding under action of controllable magnetic fields. It is shown that today different authors have various explanations of the facts of refinement of weld metal structural constituents or deposited metal in arc welding under action of a longitudinal magnetic field. There is no single opinion between the authors on the most important factors determining refinement of the weld metal structural constituents in welding under action of the longitudinal magnetic field. It is shown that peculiarities of action of the longitudinal magnetic field on formation of secondary structures in a weld during arc welding also require investigation. It is not determined what is the stage where the weld metal structure refinement takes place under the action of magnetic fields, namely during primary crystallization or during secondary transformations or simultaneously during these two stages. It is necessary to carry out investigations in this direction in order to develop the optimum parameters of the external magnetic fields for weld structure refinement in arc welding. 20 Ref., 1 Figure.

Keywords: *weld metal structure refinement, crystalline particle, external magnetic fields, refinement factor.*

It is known that reduction of grain size results in increase of metal yield strength in accordance with Hall-Petch relationship [1]. There is number of publications, in which it was determined, that arc welding under action of longitudinal magnetic fields (LMF) or transverse magnetic fields (TMF) provokes refinement of weld metal (deposit) structure and improvement of mechanical properties of welds. However, action of indicated fields in welding does not always result in weld metal refinement. The authors have different explanation of action of magnetic fields (MF) on size of structure constituents of weld metal, forming during its crystallization.

Let's consider existing ideas (hypotheses) of some authors on mechanism of weld metal structure refinement in arc welding under MF action.

It should be noted that there are fundamental works on theory of metal crystallization in process of its solidification [2, 3]. Nevertheless, these works are referred to casting processes or production of super-pure single crystalline particles. Conditions of metals crystallization, described in them, significantly differ on conditions of metal crystallization in weld pool, and they, partially, can be applied for welding process conditions.

The aim of the present work is analysis of available publications on determination of refinement mechanism of the primary and secondary weld structures under action of magnetic fields.

One of the first works [4] applicable to welding of titanium alloy OT4-1 of 1.5 mm thickness and 10 mm thickness heat-resistant austenite alloy of nimonik type under action of LMF suggests that barely visible refinement of weld structure of OT4-1 alloy is related with the fact that a crystallization front has relatively smooth surface and significant weld refinement of austenite alloy is related with the fact that the crystallization front is a mass of growing needles, chipping of which requires less energy expenses, i.e. mechanism of action is not indicated in details.

Later, these authors in their publication [5] indicated that the main value for structure refinement has diffusion processes and temperature variations of liquid phase, periodically changing a level of concentration overcooling. At that, not mechanical, but temperature variations of liquid phase in the pool are important. However, the decisive role in this case has concentration overcooling.

Work [6] determined that low-frequency vibration of the weld pool in welding does not lead to sound resonance action and cannot break growing crystals. It is assumed that the pressure waves appear in a melt.

This creates momentary temperature gradients between neighbor points in cooling melt that results in rise of dislocation number and grain refinement.

A problem on possibility of chipping of growing crystals by liquid metal moving under action of LMF (or TMF) is discussible. One of the works [7] states that such chipping takes place, and another one [8] affirms that doesn't.

Filming of the crystallization process in welding of nickel under action of LMF was carried out in work [9]. It is determined that crystallization starts on fused grains of the base metal, then displacement of flat crystallization front takes place. Accumulation of additives before the moving flat front stimulates concentration overcooling. This results in decay of this flat front and formation of cells at interphase. As a consequence, temperature balancing in weld pool volume in welding under LMF action before crystallization front rises temperature gradient [10–12].

Work [11] studies non-etched surfaces of the crystallization front detected in a splash of pool liquid metal in process of welding of titanium and its alloys. Decrease of lateral dimensions of the crystals under LMF action is found. This was also observed in submerged-arc and argon welding under LMF action of chromium-nickel steels. Welding under LMF action always rises structure homogeneity and decreases chemical inhomogeneity of weld structure. It was explained by change of crystallization kinetics, provoked by periodic variations of parameters of concentration overcooling zone before interphase depending on temperature gradient in the crystallization front. There are two semiperiods of temperature variation close to this front, namely hot and cold. During the first (hot) semiperiod the crystallization front is overheated in a pool head, liquid metal washes it and rises, at that, temperature gradient in comparison with its value in welding without LMF action. This leads to reduction of rate of crystalline particles growth, decrease of size of two-phase area, shorten extension of zone of concentration overcooling. During the second (cold) crystallization semiperiod the temperature gradient in the crystallization zone reduces to the values, lower than in welding without LMF action. At that size of concentration overcooling zone rises, crystallization accelerates, structural constituents are refined. Under action of alternating LMF the maximum crystallization rates 1.5–10.0 times exceed crystallization rate typical for welding process without LMF action. Expressed ideas of these authors are sufficiently convincing. However, to improve their reliability it is desirable to determine if there is alternation of layers of finer

and coarser crystalline particles, which by configuration should repeat the boundaries of pool end part.

Work [13] shows that fusion of solidified metal is inevitable in process of crystallization with temperature fluctuations near the crystallization front under conditions of arc welding. At that the solid phase areas having higher content of alloying elements, and, respectively, lower melting temperature, fuse in the first case. Such areas in dendrites are the bases of second order branches. In temperature fluctuations close to interphase there is separation of the dendrite branches of the main stalk. Separated dendrite branch can form new crystal without additional nucleus. During the pause (under action of alternating LMF with pauses) the crystallization front should displace for a distance equal the thickness of two-phase area. Such an approach allows getting the optimum repetition frequency and hardness of pulses of alternating LMF necessary for grain refinement. It is determined that the optimum LMF frequency is within 0.6–15.0 Hz limits that matches with recommended values of frequencies in a lot of works. It is also stated that welding of pure metals and alloys with low interval of crystallization provokes virtually no refinement of the primary crystals (in welding under LMF action). It is related with small thickness of two-phase zone and underdevelopment of axes of the second order dendrites. In our opinion this mechanism of structure refinement is possible in arc welding and surfacing when dendrite crystallization is observed most often. It is also indicted in work [12]. However, it should be taken into account, that if more fusible fragments of second order branches is taken out in hotter liquid metal of the pool before the crystallization front, than they will be melted and won't play a role of crystallization centers.

When we are talking about direction of growth of crystalline particles in the pool than for the case of arc welding without external actions it is generally accepted that this direction is described by equation proposed by V.M. Shamanin [14–16] (Figure 1, *a*):

$$v_s = v_w \cos \alpha,$$

where v_w is the welding rate, m/s; α is the angle between the direction of crystal growth in each determined moment of crystallization and direction of displacement of heat source (axis OX).

In point A angle $\alpha = 90^\circ$, i.e. rate of crystal growth v_c close to side edges of the pool equals to zero. In point C when crystal growth is completed angle $\alpha = 0$ and then v_c becomes equal welding rate. Direction of crystal axis (ABC line) is orthogonal to line AD (Figure 1, *a*).

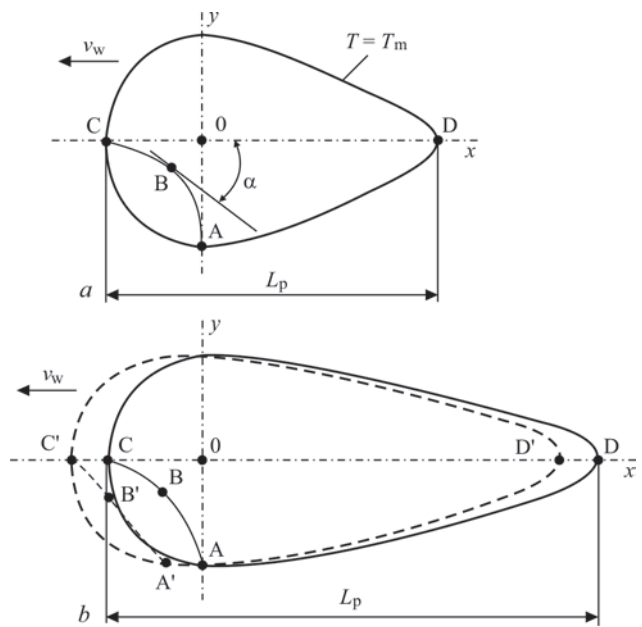
In submerged-arc welding and surfacing, when $I_w = 500\text{--}1000$ A, welding rate $v_w = 20\text{--}40$ m/h and more (as it was shown by investigation of splashes of weld pool), a pool shape corresponds to shape given in Figure 1, *b*, i.e. the pool is of significant length ($L_p = 50\text{--}100$ mm and more). The side edges of pool (close to point A) are almost parallel to axis OX . If line AD is shifted to the left with specific step (line $A'D'$ on Figure 1, *b*), points A, B, C will be also shifted with the same step (line $A'B'C'$), i.e. point A is also shifted with such a step and then crystallization rate in point A $v_c = v_w$ and the crystal in this point should grow in welding direction (axis OX) with v_w rate. In this connection it is unknown how crystals are nucleated and grow on side sections of the pool (on section AA') and dendrite (crystal) axes in this zone will be of the first or second order. Similar is in the passing point B. This circumstance is not taken into account in the formula and not considered in all cited papers and manuals mentioned above [14–16]. It requires more detailed research.

Authors of works [13] and [5] hold an opinion that the value of forces appearing in the pool under LMF action is obviously not enough for growing crystals chipping. They suppose like the authors of work [11] that the leading factor of structure refinement is concentration overcooling. The works mentioned above considered action of LMF in welding on the primary structure refinement. However, it can be assumed that the flows of liquid metal initiated in welding under LMF action influence formation (refinement) of the secondary structures.

Works [17, 18] show that LMF in arc welding effects formation of crystal boundaries. It takes place due to additional dynamic pressure on the front of growing crystals by pool molten metal that develops stresses and elastic deformations in solid phase, results in formation of significant amount of dislocations. Such a mechanism of structure refinement takes place in the opinion of authors of work [18] in welding of technically pure metals, in particular, titanium and nickel in welding under LMF action.

It is well-known fact that the welds are characterized with periodic crystallization. This fact is explained by presence of lamination in weld crystallization [14] caused by terminations of crystallization in a period of emission of crystallization latent heat.

Works [19, 20] show a laminar structure in weld crystallization during welding without external actions for superpure (and technically pure) metals, when realizing thermal overheating as well as crystallization of alloys (in presence of additives), when realizing not only thermal, but concentration overheating. It is shown that frequency of natural crystalli-



Scheme for determination of direction of crystalline particle growth: *a* — short pool; *b* — pool shape applicable to welding on forced modes

zation of welds depends on welding rate, composition of metal being welded and its thickness. The authors of works [19, 20] propose a method for weld structure refinement due to harmonization of frequency of external disturbances (including LMF action) with own crystallization frequency for getting a resonance. However, the mechanism of achievement of structure refinement at getting the resonance, outlined by the authors, in our opinion is not convincing. It is necessary to carry out additional investigations in order to prove the action of indicated mechanism of refinement of weld structural constituents.

Conclusions

1. Now there are a lot of hypotheses on mechanism of weld structure refinement under action of controllable MF. It is necessary to carry out further investigations on stating the leading factors determining refinement of weld structure in welding under MF action.

2. It has not been determined what is the stage where weld structure refinement under MF action takes place, i.e. in primary crystallization, in secondary transformations or simultaneously during these two stages. It is necessary to carry out investigations in this direction in order to develop the optimum parameters of LMF (TMF) for weld structure refinement in arc welding.

1. Lakhtin, Yu.M. (1977) *Physical metallurgy and heat treatment of metals*. Moscow, Metallurgiya [in Russian].
2. Chalmers, B. (1968) *Theory of solidification*. Moscow, Metallurgiya [in Russian].
3. Flemings, M. (1977) *Processes of solidification*. Moscow, Mir [in Russian].

4. Boldyrev, A.M., Dorofeev, E.V., Antonov, E.G. (1971) Control of crystallization of metal in fusion welding. *Svarochn. Proizvodstvo*, **6**, 35–37 [in Russian].
5. Boldyrev, A.M. (1976) On mechanism of formation of weld metal structure by introduction of low-frequency oscillations to weld pool. *Ibid.*, **2**, 53–55 [in Russian].
6. Sutyryn, G.V. (1975) Study of mechanism of impact of low-frequency vibration on crystallization of weld pool. *Avtomatich. Svarka*, **5**, 7–10 [in Russian].
7. Chernysh, V.P., Pakharenko, V.A. (1979) Kinetics of crystallization of pool in welding with electromagnetic stirring. *Ibid.*, **3**, 5–7 [in Russian].
8. Aristov, S.V., Russo, V.L. (1982) Crystallization of weld metal in low-frequency oscillations of melt. *Svarochn. Proizvodstvo*, **11**, 42–44 [in Russian].
9. Abralov, M.A., Abdurakhmanov, R.U., Kulushev, A.T. (1977) Peculiarities of crystallization of weld metal pool under electromagnetic stirring conditions. *Avtomatich. Svarka*, **8**, 7–11 [in Russian].
10. Malinkin, I.V., Chernysh, V.P. (1970) Selection of modes of welding pool electromagnetic stirring. *Ibid.*, **7**, 14–16 [in Russian].
11. Chernysh, V.P., Kuznetsov, V.D., Briskman, A.N. et al. (1983) *Welding with electromagnetic stirring*. Kiev, Tekhnika [in Russian].
12. Korab, N.G., Kuznetsov, V.D., Chernysh, V.P. (1990) Evaluation of effect of controllable magnetic field on crystallization in arc welding. *Avtomatich. Svarka*, **2**, 33–36 [in Russian].
13. Abralov, M.A., Abdurakhmanov, R.U. (1982) On mechanism of refinement of weld metal primary structure in electromagnetic action. *Ibid.*, **2**, 18–21 [in Russian].
14. Bagryansky, K.V., Dobrotina, Z.A., Khrenov, K.K. (1976) *Theory of welding processes*. Kiev, Vysshaya Shkola [in Russian].
15. (1970) *Theoretical principles of welding*. Ed. by V.V. Frolov. Moscow, Vysshaya Shkola [in Russian].
16. (1988) *Theory of welding processes*. Ed. by V.V. Frolov. Moscow, Vysshaya Shkola [in Russian].
17. Abralov, M.A., Abdurakhmanov, R.U. (1975) Kinetics of formation of secondary boundaries and propagation of hot cracks in welding of nickel. *Avtomatich. Svarka*, **22**, 31–34 [in Russian].
18. Abralov, M.A., Abdurakhmanov, R.U. (1980) Some peculiarities of formation of secondary boundaries in welds in electromagnetic impact. *Ibid.*, **2**, 12–18 [in Russian].
19. Morozov, V.P. (2006) Analysis of conditions of refined structure formation in crystallization of weld pool metal with periodic oscillation superposition. *Izv. Vuzov. Mashinostroenie*, **8**, 41–54 [in Russian].
20. Morozov, V.P. (2011) Effect of proper frequency synchronization of oscillation mechanism of weld crystallization and frequency of external periodic impact on technological strength during welding. *Nauka i Obrazovanie*, **12**, 1–14 [in Russian].

Received 13. 01.2018

INFLUENCE OF ARC SURFACING MODES ON INTERGRANULAR PENETRATION OF HIGH-TIN BRONZE INTO STEEL

T.B. MAJDANCHUK, V.M. ILYUSHENKO and A.N. BONDARENKO

E.O. Paton Electric Welding Institute of the NAS of Ukraine
11 Kazimir Malevich Str., 03150, Kyiv, Ukraine. E-mail: office@paton.kiev.ua

The paper gives the results of studying the influence of the parameters of the submerged-arc surfacing process of steel with flux-cored wire of PPBrOF10-1 grade and with coated electrodes ANBO-2, providing deposited metal of the composition, corresponding to cast bronze of BrO10F1L grade, on formation of intercrystalline penetrations of bronze into steel. It is shown that formation of intercrystalline penetrations is the most significantly influenced by values of current and deposition rate. Based on metallographic examinations, it is found that absence of intercrystalline penetrations of bronze into steel is achieved at limitation of efficient heat input of the arc surfacing process both with flux-cored wire and with coated electrodes to the value of 450 kJ/m. 8 Ref., 2 Tables, 2 Figures.

Keywords: *high-tin bronze, coated electrodes, flux-cored wire, arc surfacing, intercrystalline penetrations*

The high-tin bronzes find a wide application in friction units operating under particularly severe conditions at high loads [1, 2]. Thus, for example, tin-phosphorous bronze BrO10F1L is applied in the power engineering for manufacture of bearing bushings and pistons of critical purpose. This is largely contributed by the favorable combination of its mechanical and antifriction properties, which is due to a specific structure consisting of α -solid solution, eutectoid ($\alpha + \delta$), and copper phosphides [1, 2]. With the aim of saving the scarce and expensive bronze, as well as improving the structural strength of parts, the use of steel-bronze bimetal is challenging. In many cases, this problem can be solved by applying the arc methods. The limiting factor for arc surfacing of high-tin bronzes is the absence of electrode materials (wires, strips), which provide the necessary chemical composition of deposited metal. In connection with the need in producing bimetal steel + high-tin bronze, at the E.O. Paton Electric Welding Institute the flux-cored wire of grade PPBrOF10-1 (recommended for automatic surfacing) and coated electrodes of grade ANBO-2 [3, 4] were developed. These materials were developed taking into account the requirements to provide producing of the deposited metal, corresponding by the composition to the cast bronze of grade BrO10F1L.

As is known, among all the copper alloys the tin bronzes are most prone to the formation of intercrystalline penetrations (ICP) of bronze into steel (during deposition on steel and welding of bronze with steel), which lead to a decrease in the impact strength, ductility, strength of bimetallic joints of bronze with steels

at dynamic and cyclic loads [5–7]. Figure 1 shows the characteristic form of this defect during deposition of high-tin phosphorous bronzes on steel.

As a result of metallographic examinations, it was established that ICP of high-tin bronze into steel along the entire length have a cast structure and form a tight metallic joint with steel. The penetrations begin at the fusion line of copper alloy-steel and penetrate into steel along the grain boundaries. They pass along several grain boundaries, have different width and length. One and the same penetration as to its length can have areas with the same or variable width; the boundaries



Figure 1. Microstructure ($\times 50$) of metal of fusion zone of high-tin bronze and steel with ICP of bronze into steel

Table 1. Influence of modes of surfacing using flux-cored wire PPBrOF10-1 under flux and efficient heat input on tendency to formation ICP of bronze into steel

Number of specimen	Surfacing modes	Efficient heat input, kJ/m	Bead sizes, mm			ICP	
			Width	Height	Penetration depth	Section I	Section II
Current, A							
1	200–220	447.2	14.5–15.5	4.5–5.0	≤ 0.2	Absent	Absent
2	300–320	602.4	20–20.5	5.0–5.5	1.5–2.5	2	Absent
3	380–400	777.6	24–25	5.3–5.5	1.5–2.5	1	2
Voltage, V							
4	25–26	430.9	14.5–15	5.5–6.0	1.0;1.5	Absent	Absent
5	30–31	518.4	16.5–17	5.0–5.5	0.5;1.0	Same	2
6	35–36	602.6	19.5–20	5.0–5.2	2.5;1.5	2	Absent
V_d , m/h							
7	10	842.4	20–21	5.0–5.5	≤ 0.5	3	2
8	14	602.4	19.5–20	5.0–5.2	2.5–1.5	2	Absent
9	18	369.4	18–18.5	4.0–4.5	≤ 0.5	Absent	Same

of one and the same penetration at separate areas can be parallel, but can also pass at an angle to each other.

The mechanism of ICP of copper alloy into steel during arc surfacing was rather well studied in the works [5–8]. At the same time, there are comparatively few works devoted to the study of technological measures for preventing ICP. Most often for these purposes, it is recommended to apply deposition of a sublayer of materials not prone to ICP formation (alloys with a high-nickel content, such as monel, etc.).

The data given in the literature on the effect of surfacing and heat input modes on formation and development of ICP bear a recommendatory nature, and in most cases refer to the processes of surfacing in shielding gases.

The data on the effect of modes of surfacing under flux and using coated electrodes of any copper alloys

on ICP are absent. Therefore, to evaluate the effect of submerged-arc surfacing modes on ICP using the developed flux-cored wire PPBrOF10-1 and coated electrodes of grade ANBO-2, a complex of investigations was performed. In each experiment, one process parameter was changed, while others remained constant. The flux-cored wire of 3 mm diameter, flux of grade AN-60 and coated electrodes of 3 and 4 mm diameters were used.

The efficient heat input was determined by the formula:

$$Q_{\text{eff}} = 0.24 \frac{U_a I_w \eta_{\text{eff}}}{v_d},$$

where U_a is the voltage, V; I_w is the current, A; η_{eff} is the efficiency coefficient of the process of heating the product by a welding arc (for submerged arc welding

Table 2. Influence of modes of surfacing using coated electrodes ANBO-2 and efficient heat input on tendency to formation ICP of bronze into steel

Number of specimen	Surfacing current, A	Efficient heat input, kJ/m	Bead sizes, mm			ICP	
			Width	Height	Penetration depth	Section I	Section II
$U_a = 23-25 \text{ V}; v_d = 3 \text{ m/h}$							
1	60	331	5–7	1.5–2.5	≤ 0.1	Absent	Absent
2	80	442	7–9	2.5–2.8	≤ 0.2	Same	Same
3	100	553	10–12	2.8–3.2	≤ 0.25	»	1
4	120	663	11–14	3.2–3.5	0.5	2	1
5	160	885	15–18	3.4–3.7	1.0	2	3
$U_a = 23-25 \text{ V}; v_d = 4 \text{ m/h}$							
6	60	248	5–6	1.5–2	≤ 0.1	Absent	Absent
7	80	332	6–8	2–2.5	≤ 0.15	Same	Same
8	100	415	8–10	2.5–2.7	0.5	»	»
9	120	498	11–13	2.8–3.1	0.8	»	1
10	160	664	14–15	3–3.2	1.5	1	2
$U_a = 23-25 \text{ V}; v_d = 5 \text{ m/h}$							
11	60	200	4–5	1–2	≤ 0.1	Absent	Absent
12	80	265	5–6	2–2.2	≤ 0.2	Same	Same
13	100	331	7–8.5	2.2–2.5	0.5	»	»
14	120	398	9–11	2.5–2.8	1.5	»	»
15	160	531	10–13	2.8–3	2.0	2	»

$\eta_{\text{eff}} = 0.8\text{--}0.95$, for coated electrode, $\eta_{\text{eff}} = 0.65\text{--}0.8$); v_d is the rate of deposition, m/h.

The presence and nature of ICP were studied on etched sections of specimens taken from the cross-section of the bead (not less than two areas). The sizes of cross-section of the beads and the penetration depth of base metal were also fixed. The results of investigations are given in Table 1.

From the results presented in Table 1, it is seen that appearance of ICP is affected by all the parameters of surfacing process. However, the current value and the deposition rate have a greater influence than the arc voltage. Any effect of the penetration depth on ICP was not revealed. ICPs are also equally probable during penetration (up to 2.5 mm) and almost at its complete absence (≤ 0.5 mm) — deposited specimens 3 and 7. The heat input in these cases is approximately the same. It is also seen from Table 1 that there is a certain threshold value of the efficient heat input, below which the ICP formations are low probable. For the process of surfacing under flux using the flux-cored wire PPBrOF10-1, this value is 450 kJ/m.

During deposition on steel using coated electrodes, the value of the efficient heat input mainly depends on the value of current and deposition rate. The results of carried out investigations are given in Table 2.

The data presented in Table 2, indicate that the value of the efficient heat input of 450 kJ/m is a critical value, exceeding which the ICPs of bronze into steel in the deposited metal are present. Therefore, during deposition on steel (especially of the first layer), it is rationally to use coated electrodes of 3 mm diameter. In this case, a more stable process without the arc breaks and short circuits of the electrode on the steel plate is provided.

The microstructure of the metal in the fusion zone of high-tin bronze with steel deposited at the modes $U_a = 23\text{--}25$ V; $v_d = 4$ m/h; $I_w = 80\text{--}100$ A using electrode of grade ANBO-2 of 3 mm diameter is shown in Figure 2.

The metallographic examinations revealed no defects, including ICP of bronze into steel in the fusion zone.

As a result of carried out experimental works it was established that by limiting the efficient heat in-

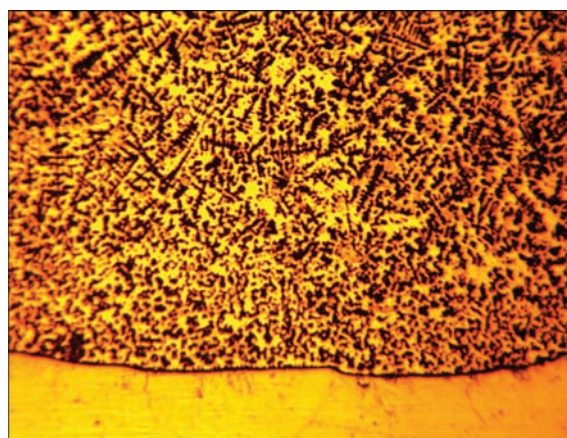


Figure 2. Microstructure ($\times 50$) of metal of fusion zone steel + high-tin bronze

put of arc methods of deposition of high-tin bronze on steel below 450 kJ/m, it is possible to minimize the probability of formation and significant development of ICP using flux-cored wire PPBrOF10-1 and ANBO-2 coated electrodes as electrode materials.

1. Osintsev, O.E., Fedorov, V.N. (2004) *Copper and copper alloys. National and foreign grades: Handbook*. Moscow, Mashinostroenie [in Russian].
2. Davis, J.R. (2001) *Copper and copper alloys. ASM Int.*
3. Ilyushenko, V.M., Majdanchuk, T.B., Bondarenko, A.M. et al. *Flux-cored wire for welding and surfacing of high tin bronze*. In: Author's cert. 109622 UA. Int. Cl. B23K 35/16 (2006.01) [in Ukrainian].
4. Ilyushenko, V.M., Majdanchuk, T.B., Anoshin, V.O., Skoryna, M.V. *Composition of electrode coating for welding and surfacing of tin bronze*. In: Author's cert. 106954 UA. Int. Cl. B23K 35/365 (2006.01) [in Ukrainian].
5. Rybin, V.V., Vajnerman, A.E., Baranov, A.V. et al. (2006) Investigation of peculiarities and development of advanced technologies of welding of copper alloys with steels and surfacing of copper alloys on steel. *Voprosy Materialovedeniya*, **1**(45), 220–229 [in Russian].
6. Ardentov, V.V., Vajnerman, A.E., Zakharov, V.F. et al. (1979) Influence of penetration of copper alloy in steel on properties of bimetal. *Avtomatich. Svarka*, **5**, 36–38 [in Russian].
7. Vajnerman, A.E., Pichuzhkin, S.A., Chernobaev, S.P. et al. (2006) New welding consumables and technological peculiarities of welding and surfacing of products from copper alloys and dissimilar metals. In: *Proc. of Int. Sci.-Techn. Conf. on Welding Consumables – 2012*, 141–147.
8. Vajnerman, A.E. (1981) Mechanism of intercrystalline penetration in surfacing of copper alloys on steel. *Avtomatich. Svarka*, **6**, 22–25, 29 [in Russian].

Received 10.02.2018

ELECTROSLAG SURFACING WITH LARGE-SECTION ELECTRODE AT DIRECT CURRENT IN CURRENT-SUPPLYING MOULD

Yu.M. KUSKOV, V.G. SOLOVIOV, P.P. OSECHKOV and V.V. OSIN

E.O. Paton Electric Welding Institute of the NAS of Ukraine
11 Kazimir Malevich Str., 03150, Kyiv, Ukraine. E-mail: office@paton.kiev.ua

The influence of different circuits of electrode connection to one or two DC power sources on base metal penetration at electroslag surfacing of end faces was studied. It is established that the circuits of electrode connection both to one and two DC power sources can be used to obtain minimum and uniform penetration. Shortening of the distance from the processed surface (billet end face) to the current-conducting section of current-supplying mould leads to an increase of surfacing efficiency and reduction of specific power consumption. 12 Ref., 1 Table, 3 Figures.

Keywords: *electroslag surfacing of end faces, large-section electrode, current-supplying mould, DC power sources, processed surface, base metal penetration*

Alternating current of commercial frequency is traditionally used for powering electroslag furnaces (processes of electroslag remelting (ESR), electroslag casting (ESC)), welding and surfacing units (processes of electroslag welding (ESW) and electroslag surfacing (ESS)) [1, 2]. For furnaces this choice is due to simplicity of electrical equipment and high quality of the produced metal. For welding-surfacing units the determinant factor also is the lower cost and simplicity of electrical equipment. Here, for instance, the stability of ESW process at alternating current is not worse than that at direct current, and in the case of operation at direct current at its large values, electrolysis phenomena proceeding in the slag pool, may disturb process stability.

However, direct current was quite extensively used abroad at the initial stage of ESR development. And at present both combined current with superposition of direct current on alternating current, and purely direct current of different polarity can still be used for different reasons (production, metallurgical and economic) [3–7]. In [6] some features of electroslag process at direct current are generalized. It was necessary to check the advantages of direct current (depending on polarity), compared to alternating current, at ESS in a current-supplying mould (CSM).

This work is a continuation of investigations of ESS of end faces by large-section electrodes (40–130 mm diameter), using CSM of 180 mm diameter [8, 9]. Its objective is evaluation of the prospects for direct current application at ESS, when using one or two sources and different circuits of connection of the electrode, item and current-conducting section of

the mould. Metallurgy of electroslag process at direct current was not considered in this paper.

Procedure of experiment performance differed from that accepted in [9] by that the experiments were performed only with 90 mm electrode at liquid start, and power sources were VDU-1202 and VDM-5000. Measurement, as well as recording of currents and voltages, was conducted using equipment and software indicated in [9]. Figure 1 shows the structural diagram of electrical connections during performance of experiments for one-loop (*a, b*) and two-loop (*c*) ESS.

First of all, before the start of experiment performance, it was necessary to more precisely determine the possibility of CSM operation at reverse polarity. Already at the beginning of investigation of electroslag process in a standard mould, it was established [10] that at application of nonconsumable water-cooled copper electrode and fluxes of different chemical composition a stable process was observed only in the case, when the electrode was the cathode (straight polarity). The process at reverse polarity could only be realized using slags, not containing SiO_2 , in particular, with chemically pure CaF_2 . However, in this case, an intensive destruction of the electrode surface was observed. At application of a carbon electrode, the process stability did not differ from that found at melting of consumable metal electrodes (steel, copper, tungsten, molybdenum, etc.).

It should be noted that one of the developers of CSM design also states that the current-supplying mould can be operated only at applying straight polarity direct current to it. At reverse polarity the electroslag process is gradually phasing out [11]. As one

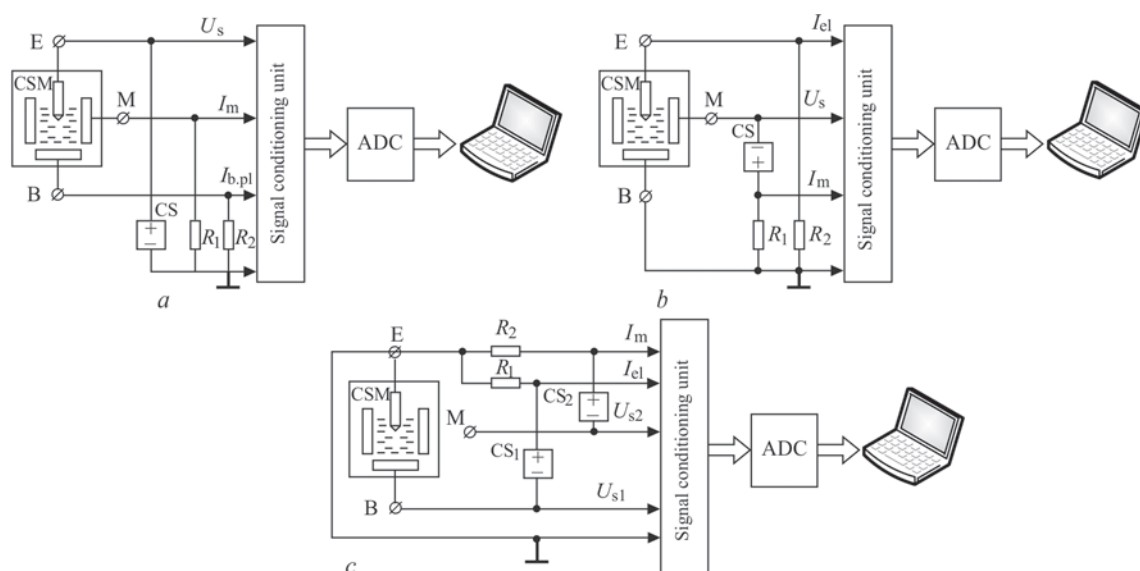


Figure 1. Structural diagram of electrical connections for performance of experimental surfacing for one-loop (*a*, *b*) and two-loop (*c*) ESS: E, M, B are the terminals of connection of the electrode, mould current-conducting section and bottom plate with the item, respectively; CS (CS1 and CS2) is the direct current source; R_1 and R_2 are the measuring current shunts; U_s (U_{s1} and U_{s2}), I_m , $I_{b,pl}$ and I_{el} are the signals proportional to current source voltage, mould, bottom plate and electrode current, respectively; ADC is the analog-digital converter

can see, there is a certain contradiction between the data in [10, 11]. In the first case, the electroslag process with carbon electrode is stable at direct current of any polarity, similar to consumable electrode melting. Now, in the case of application of CSM, the copper current-conducting section of which is protected by graphite (carbon) lining, through which current flows into the slag pool, the process at reverse polarity is not only not stabilized, but even stops.

In view of the fact that during setting the slag pool in the mould, the solid start is also used in a number of cases, alongside the liquid one, the electroslag process was studied under the conditions, when the water-cooled electrode (with a graphite attachment at its working end face) and CSM current-conducting section (having a graphite protective lining) were the anode and cathode relative to the bottom plate with the billet, respectively. VDM-5000 power source and ANF-29 flux not applied earlier in the above mentioned works, were used in the experiments.

The experiment with water-cooled electrode and graphite attachment was conducted by setting a slag pool in the CSM forming section, without applying voltage to its current-conducting section, i.e. CSM in this experiment was a standard mould. The slag pool was set only at the attachment surface in the form of a ring approximately 30 mm wide and even at increase of thermal power applied to the pool, this zone did not essentially change its dimensions. In addition, microarcs, similar to those described in [10], were observed on the upper interphase of slag — attachment surface around the entire perimeter. The process had to be stopped. Examination of the attachment working

part showed the following. A band about 5 mm wide and 3–5 mm deep formed on its end face. Here, that entire «trench» is covered by small pits, which, obviously, are the sites of microarc appearance. Now in the region, where the microarcs were observed on the slag surface, no visible changes were found on the attachment surface. Schematic of attachment wear and its appearance after testing are shown in Figure 2.

Testing CSM serviceability at reverse polarity was performed by pouring molten slag overheated in a separate tank, inside the same mould, but with voltage application to its current-conducting section. Already a few seconds after pouring, the slag pool started cooling down; bright glow and some movement of slag were noted just in its local zones. Then, pool cooling occurred over its entire surface with current lowering to zero.

Thus, neither the water-cooled graphite electrodes, nor CSM current-conducting sections, having a pro-

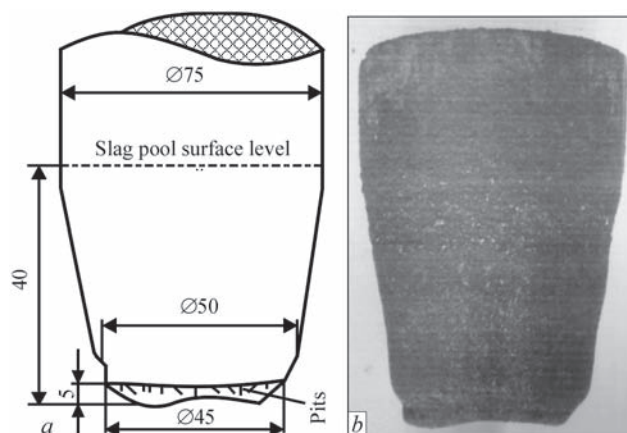


Figure 2. Schematic of attachment wear (*a*) and its appearance after testing (*b*)

Parameters of electroslag surfacing of end faces in CSM at direct current

Experiment number	Electrode diameter, mm	Connection circuit	Current, kA		Voltage, V			N_t , kV·A	N_m/N_t , %	V_{el} , mm/min	G , kg/h	h , mm	Q , kW·h/kg	Surfacing quality		
			C	E	C	E	B							H_{av} , mm	Δ_{av} , mm	PSFQ
45M	90	OLC1	2.3	2.6	0	43	0	110	88	34	83	44	1.3	1	0.8	Satisfactory
46M	90	OLC2	2.94	1.09	0	36	36	106	100	14	21	44	5	3	2	Good
47M	90	TLEI	0.74	1.87	6	62	0	111	40	42	69	44	1.6	1	0.8	Good

Note. OLC1 and OLC2 are the one-loop circuits of CSM connection, the first with the same potentials at the item and CSM current-conducting section, the second with the same potentials at the item and electrode, respectively; TLEI is the two-loop circuit of CSM connection with a common point of connection on the electrode; N_t is the total power consumed by CSM; N_m/N_t is the ratio of power at the mould and the total power; V_{el} is the linear speed of electrode movement; G is the surfacing efficiency; h is the distance from the processed surface to the forming section top; Q is the specific power consumption; H_{av} is the average penetration depth; Δ_{av} is the average nonuniformity of penetration; PSFQ is the processed surface formation quality (expert evaluation).

tective graphite lining, allow conducting a stable electroslag process at reverse polarity.

Proceeding from the obtained results, surfacing in CSM should be performed at straight polarity. However, some explanation of the terminology is required. In welding science it is customary to evaluate polarity in a relative form [12]. This implies existence of the following relationships: if voltage is applied to the item from power source (+) terminal, and to the electrode — from (–) terminal, then polarity is considered to be straight. In case of reverse connection, reverse polarity is in place. In [6] the features of electroslag process at different polarity are considered exactly proceeding from such a connection to the power source.

Now, if during the electroslag process the slag pool is in contact not with one, but with two electrodes (consumable electrode and CSM current-conducting section), there arises an uncertainty at assessment of the type of mould connection relative to the consumable electrode. In order to eliminate this uncertainty, at further consideration of various electric circuits of connection of the source (sources), we will use just (+) or (–) symbol designations, without specifying the surfacing process polarity.

The Table gives the results of experiments on investigation of the influence of electric parameters of the process of ESS at direct current in CSM (at application of different schematics of its connection) on base metal penetration.

Three experiments with one-loop OLC1 (Figure 1, a), and OLC2 (Figure 1, b) circuits and with two-loop TLCEI (Figure 1, c) circuit of current source connec-



Figure 3. Macrosection of bimetal billet from experiment 45M

tion were performed. Here, preliminary experiments on ESS with OLC1 circuit with electrode connection to terminal (–), as well as OLC2 circuit with CSM current-conducting section connection to (+) terminal, showed negative results, the process was sluggish with its phasing out that is associated with the presence of a «valve effect» at ESS. Therefore, experiments 45M and 47M were performed with consumable electrode connection to terminal (+).

It was established that samples produced in experiments 45M and 47M have, practically, the same indices of surfacing quality. Here, in the sample from experiment 45M the values of efficiency and specific power consumption are somewhat better. More over, TLCEI circuit (Figure 1, c) is more complex to implement, because of availability of two power sources. It follows that electroslag surfacing of end faces at direct current with one-loop circuit of connection to the current source, is preferable, compared to two-loop circuit. Figure 3 shows the macrosection of a bimetal sample from experiment 45M.

From the three conducted experiments, experiment 46M showed the worst results, both as to process efficiency, and as to specific power consumption. Experiment with OLC2 circuit (compared to OLC1) leads to 4 times reduction of G , 3.8 times increase of Q , increase of H_{av} from 1 to 3 mm and of Δ_{av} from 0.8 up to 2.0 mm. Such results are attributable to the fact that the highest current equal to a sum of currents at the electrode and the item, flows through CSM. Due to that, the fraction of power consumed for electrode melting and metal pool heating, decreased, while efficiency dropped and power consumption increased, respectively. The results of experiment 46M with the circuit with the same potentials at the billet and the electrode, lead to the conclusion that surfacing with such a connection circuit should not be used for high-quality ESS.

It is interesting to compare the results of experiments, conducted with application of an alternating

current source [9] and direct current source with the same connection circuits and with the same electrode diameters, but with different arrangement of the processed surface, relative to the top of the forming section. Experiment 22M [9] was conducted with $h = 85$ mm, and 45M with $h = 44$ mm. Two times reduction of the distance between the processed surface and forming section top led to increase of ESS process efficiency 1.7 times, and reduced power consumption 1.8 times, value of average penetration depth of base metal from 7 to 1 mm and value of average non-uniformity of penetration from 3.0 to 0.8 mm.

Work [9] analyzed the prospects of studying ESS by the two-loop power circuit with a common point of connection of both the sources on the electrode, presumably having a higher efficiency than the circuit with a common point of connection on the item. In this work, experiment 47M was conducted with connection of two direct current sources, having a common point of connection on the electrode (Figure 1, c). The consumable electrode and CSM current-conducting section are connected to (+) terminals.

The potential at the electrode with respect to the item is +62 V (see Table), and on the mould current-conducting section it is +6 V, respectively. On the mould current-conducting section the potential relative to the electrode is equal to -56 V, i.e. the current practically does not flow through the mould current-conducting section to the item that, in our opinion, should lower the effectiveness of the process with this circuit of source connection. We performed experiment 25M [9] with connection of two alternating current sources, having a common connection point on the item. Electrode voltage was approximately 68 V, voltage of the mould current-conducting section was about 37 V. Comparison of the results of the considered experiments reveals the advantage of ESS process at direct current. So, experiment 47M, unlike 25M, shows an increase of process efficiency, reduction of specific power consumption and improvement of fusion quality. This is, supposedly, related to the fact that an increased near-anode potential drop is created at the electrode, which is the anode that promotes an increase of electrode melting rate. In addition, 1.13 kA current flows through the item (current on the electrode, minus current on the mould). This is equal to 60 % of total current flowing through the electrode that promotes good fusion of the base and deposited metals.

Conclusions

1. Possibility of performance of ESS of end faces at different electric circuits of electrodes connection

from one or two DC power sources was established and influence of electric and process parameters on base metal penetration was studied.

2. It was established that the circuits of electrode connection both to one and two DC power sources can be applied, in order to achieve a minimum and uniform penetration. However, surfacing at DC current with two-loop circuit of connection of power sources, compared to one-loop circuit, is less preferable, because of the complexity of its realization (presence of two power sources).

3. Shortening of the distance from processed surface (billet end face) to CSM current-conducting section leads to an increase of surfacing efficiency and to reduction of specific power consumption.

4. Experiments showed that ESS at direct current with the circuit with the same item and electrode potentials does not allow achieving high-quality surfacing.

5. As was assumed in [9], ESS with a two-loop power circuit with a common point of connection of both the sources on the electrode has a higher efficiency and lower specific power consumption, than that with a common point of source connection on the item.

6. Obtained results can make up a data bank for construction of a system of automatic regulation of base metal penetration at ESS of end faces.

1. (1976) *Electroslag furnaces*. Ed. by B.E. Paton et al. Kiev, Naukova Dumka [in Russian].
2. (1980) *Electroslag welding and surfacing*. Ed. by B.E. Paton. Moscow, Mashinostroenie [in Russian].
3. (1982) *Electroslag technology abroad*. Ed. by B.E. Paton et al. Kiev, Naukova Dumka [in Russian].
4. Chen, Ch.S., Gao, R.F. (1989) Investigation of electroslag remelting in composite mold with lined upper section. *Problemy Spets. Elektrometallurgii*, **4**, 42–47 [in Russian].
5. Latash, Yu.V., Matyakh, V.N. (1987) *Modern methods of production of especially high quality ingots*. Ed. by B.E. Paton et al. Kiev, Naukova Dumka [in Russian].
6. Mironov, Yu.M. (2002) Effect of current type on processes in electroslag installations. *Elektrometallurgiya*, **4**, 25–32 [in Russian].
7. (1986) *Metallurgy of electroslag process*. Ed. by B.E. Paton et al. Kiev, Naukova Dumka [in Russian].
8. Kuskov, Yu.M., Soloviov, V.G., Zhdanov, V.A. (2017) Electroslag surfacing of end faces with large-section electrode in current-supplying mould. *The Paton Welding J.*, **12**, 29–32.
9. Kuskov, Yu.M., Soloviov, V.G., Osechkov, P.P., Osin, V.V. (2018) Electroslag surfacing of billet end faces with application of consumable and nonconsumable electrodes. *Ibid.*, **2**, 38–41.
10. Dudko, D.A., Rublevsky, I.N. (1958) Effect of current type and polarity on metallurgical processes in electroslag welding. *Avtomatich. Svarka*, **3**, 69–78 [in Russian].
11. Ksyondzyk, G.V. (1975) Current-supplying mold providing rotation of slag pool. *Spets. Elektrometallurgiya*, **27**, 32–40 [in Russian].

Received 07.10.2017

ON THE PROBLEM OF HEAT TREATMENT OF WELDED JOINTS OF RAILWAY RAILS

E.A. PANTELEYMONOV

E.O. Paton Electric Welding Institute of the NAS of Ukraine
11 Kazimir Malevich Str., 03150, Kyiv, Ukraine. E-mail: office@paton.kiev.ua

The peculiarities of design of inductors with magnetic cores, used in a portable module for heat treatment of railway rail welded joints, produced by flash-butt welding, are presented. It is shown that the shape of the inductive wire of inductors, the location of magnetic cores relative to the rail and the technology of induction heating by currents of 2.4 kHz frequency provide a uniform distribution of temperature field in a welded joint, low temperature drop between the surface and deep layers of the rail, and also a decrease in the heating time. As a result of heat treatment of welded joints of rails R65 of steel K76F and rails UIC 60 of steel 900A in a portable module of the E.O. Paton Electric Welding Institute (PWI), the microstructure of metal of welded joints changes significantly, the hardness HRC is uniformly distributed over the width of HAZ, the deviation of hardness HRC from the level of base metal decreases. 7 Ref., 2 Tables, 6 Figures.

Keywords: rails, welded joints, heat treatment, inductors, microstructure, hardness distribution

During heat treatment (HT) of welded joints of railway rails, made by flash-butt welding, the technology of induction heating of welded joints by high-frequency currents is applied, followed by quenching of running surface of the rail head by a compressed air. The HT technology should provide structural zonal homogeneity of welded joints, leveling metal hardness and elimination of unfavorable diagram of inner residual stresses [1, 2]. For HT of rail welded joints in the workshop and track conditions in the machines of type UIN-001 of different modification [3], the current frequency of 8.0–16.0 kHz of the induction heating source was used. The heating of welded joints of rails of type R65 to the temperature of 850–950 °C from welding heat is performed in the period of 240 s. The machines are considered to be resource-saving from the point of view of power of the induction heating source [4]. The portable module of the machines UIN-001, designed for carrying out HT in the track conditions, does not require special drives and mechanisms for its arrangement to the site of welded joint and moving along the rail [5].

However, the arrangement of inductive wires of inductors along the rail in the machines UIN-001 leads to unjustified increase in the width of heat-affected zone (HAZ), and therefore, to the increase in heating time of welded joints. A long heating time at HT of rail joints in the conditions of rail welding enterprises slows down the production rate of rail sections.

To reduce the heating time of welded joints and to decrease the temperature drop between the surface and deep layers of the rail, it is rational to reduce the current frequency. At the PWI, the model of a portable module for HT of welded joints of railway rails by currents of 2.4 kHz was tested. A distinctive feature of

a portable module is the use of inductors with magnetic cores. The inductive wire of the inductor is oriented across the rail, it reproduces the bending of its surface and is made with an increased air gap above the web and tongues of the rail. The width of the inductive wire exceeds the width of the HAZ of welded joints. The magnetic cores are installed above the running surface of the head, side edges of the head, the web and the lower surface of the rail flange [6, 7]. Thus, the complex shape of the rail surface is taken into account, the magnetic coupling of the inductor-part system is improved and the necessary power distribution among the elements of the rail is achieved. A part of the power transferred to the head and to the flange is increased as compared to the web, and it decreases into the rail tongues, preventing their overheating.

In the present work the results of testing the portable module at HT of welded joints of rails R65 of steel K76F and rails UIC60 of steel 900A are presented. The quality of HT was determined on the basis of the results of metallographic examinations of butt joints after welding and after HT. The heating of joints was carried out at the power of induction heating source being 90 kW. The initial temperature of joints was 20 °C. The heating time of welded butt joints was 180 s, which is much shorter than the time, accepted in the machines of UIN-001 type. During this period, the temperature in the plane of a butt joint reached the following values: on the surface of the running head it is 900–920 °C; at a depth of 24 mm from the running surface of the head it is 850 °C; at the center of the web it is 870 °C; at a depth of 12 mm from the bottom of the flange it is 840 °C. The time for heating the running surface of the head up to the temperature of magnetic transformations was 50 s. After HT, the welded joints were cooled in calm air.

Table 1. Grain number of metal of welded joints of rails R65 after welding and after HT

Rail element	Grain number after welding			Grain number after HT			Base metal
	Joint line	5 mm from the joint line	Zone of a partial recrystallization	Joint line	5 mm from the joint line	Zone of a partial recrystallization	
Head	2-3	4-5	6-7	7-8	6	7	7-8 (5-6)
Neck	3	5	7	7-8	6-7	7	6
Foot	3	5	7	7-8	6	7	5-6

The metallographic examinations of welded joints were carried out at a depth of 24 mm from the running surface of the head, in the center of the web and at a depth of 12 mm from the flange bottom. The microstructure of metal across the width of the HAZ and the distribution of the Rockwell integral hardness (*HRC*) were determined. The polished surfaces of the specimens for investigation coincided with the axis of symmetry of the rail transverse plane. Along the rail, the surface covered the base metal and the HAZ width. To reveal the microstructure, the method of chemical etching was used in a 4 % alcohol solution of nitric acid. The size of the metal grain was determined in accordance with GOST 5639–82. The integral hardness *HRC* was measured in the durometer TK-2M at a load of 150 kg.

As investigations showed, the microstructure of base metal of rails R65 represents sorbite. There are regions with a grain number of 5–6 and 7–8 (Table 1). After welding, the width of the HAZ of joints was 37–40 mm. The microstructure of the metal along the joint line (Figure 1, *a*) consists of sorbite and narrow fringes of ferrite along the grain boundaries. The grain is rather coarse, the grain size corresponds to the number 2–3 (Table 1). In the zone of a coarse grain, at a distance of 5 mm from the joint line (Figure 1, *b*), an almost pure sorbite structure with a grain number 4–5 occurs. In the zone of a partial recrystallization, at a distance of 18–20 mm from the joint line, a significant refinement of a sorbite grain to a number 6–7 is observed. After HT of welded joints the HAZ width was 55–60 mm. The microstructure of metal across the width of HAZ was noticeably refined. Along the joint line (Figure 1, *c*) it consists of separate precipitations of sorbite and ferrite. The amount of ferrite increased. The grain number is 7–8. At a distance of 5 mm from the joint line (Figure 1, *d*), the grain number is 6–7. The similar microstructure is at a distance of 18–20 mm from the joint line. The microstructure of metal in the zone of a partial recrystallization, at a distance of 30 mm

from the joint line does not differ from the specimens after welding. The grain number is 7.

The diagrams shown in Figure 2 reflect the character of distribution of the integral hardness *HRC* along the rail after welding and after HT. In the joints after welding (Figure 2, *a*), the hardness along the joint line in the head is *HRC* 31, which is higher than the level of the base metal (*HRC* 27–28). In the web and in the flange the hardness along the joint line is *HRC* 26–28. In the rail head, at a distance of 4–6 mm from the joint line, the hardness increased to *HRC* 35. In the zone of a partial recrystallization, at a distance of 20 mm from the joint line, the hardness decreased to *HRC* 23–24. After HT of welded butt joints the change in the structure of metal led to change in hardness (Figure 2, *b*). Along the joint line it approached the level of base metal. In the head and web the hardness *HRC* is 26–28, in the flange it is *HRC* 25. The hardness in the zone of a coarse grain in the head is *HRC* 32–33. Further, up to the zone of a partial recrystallization, the hardness was stabilized up to the level of *HRC* 33, which is higher than the level of base metal. The hardness at a distance of 20 mm from the joint line changed from *HRC* 23–24 (after welding) to the level of *HRC* 33 (after HT). In the zone of a partial recrystallization, at a distance of 30–35 mm from the joint line, the hardness did not differ from butt joints after welding. A uniform distribution of the temperature field in the welded joints of rails should be noted. The level of hardness at the places of the head-to-web transition (at a depth of 40 mm from the head running surface) and web-to-flange transition (at a depth of 25 mm from the flange bottom surface), in the problem places for induction heating by high-frequency currents, corresponds to the hardness level in the head, in the web and in the flange of the rail.

After HT of welded joints, the deviation of hardness *HRC* from the level of the base metal decreased

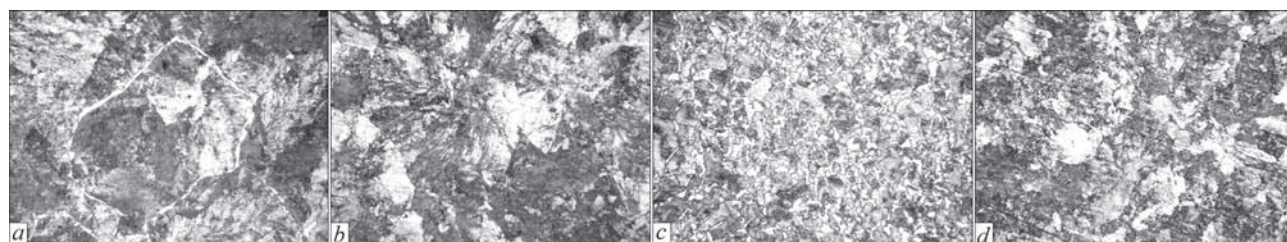


Figure 1. Microstructure ($\times 500$) of metal of welded butt joints of rails R65: joint line (*a*, *c*); at a distance of 5 mm from the joint line (*b*, *d*); after welding (*a*, *b*); after HT (*c*, *d*)

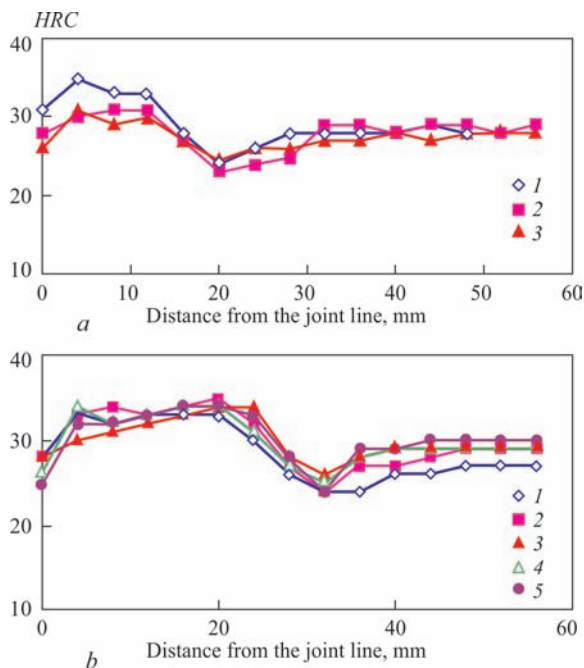


Figure 2. Distribution of hardness *HRC* across the HAZ width of welded butt joints of the rails R65: *a* — after welding (1 — head; 2 — web; 3 — flange); *b* — after HT (1 — center of the head; 2 — head-to-web transition; 3 — center of the web; 4 — neck-to-flange transition; 5 — center of the flange)

(Figure 3). In particular, along the joint line in the rail head, the deviation of hardness decreased from 10 % (after welding) to 3 % (after HT), in the zone from 5 to 20 mm to the joint line — from 20 to 13 %. In the zone of a partial recrystallization, the hardness deviation is 17 % (after welding) and 18 % (after HT).

In the rails of UIC60 type of steel 900 A, the microstructure of base metal is sorbite with a grain number 5-6 (Table 2). The changes in grain number were not revealed. After welding, the width of the HAZ of butt joints was 40–42 mm. The microstructure of the metal in the joint line (Figure 4, *a*) consists of a mixture of sorbite-like and lamellar pearlite. The thin interlayers of ferrite along the grain boundaries, as well as separate areas of ferrite component are revealed. The grain number is 2-3. At a distance of 5 mm from the joint line (Figure 4, *b*), in the zone of a coarse grain, the microstructure of the metal in the head and in the flange is sorbite, in the web it is sorbite and sorbite-like pearlite. The grain number is 4-5. In the zone of a partial recrystallization, at a distance of 18–20 mm from the joint line, a significant refining of sorbite structure in the head to the number 7-8, in the web the refining of

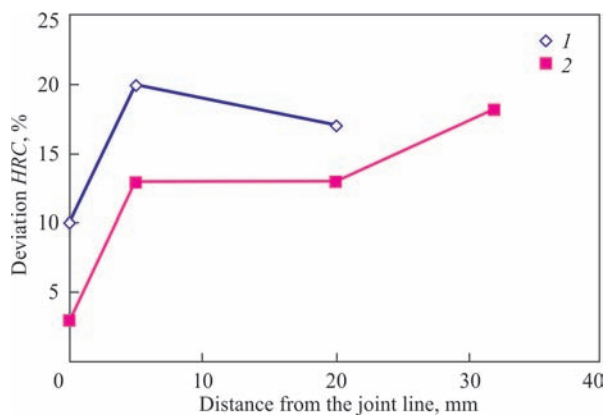


Figure 3. Deviation of hardness *HRC* in the head of the welded butt joints of the rails R65 from the level of the base metal after welding (1) and after HT (2)

sorbite-like pearlite to number 9-10 are observed. After HT of rail welded joints, the width of the HAZ in the head and in the flange is 64 mm and in the web it is 58 mm. The microstructure of metal along the joint line (Figure 4, *c*) represents a fine-grained sorbite structure with precipitations of ferrite component along the grain boundaries. In the flange there are noticeably less ferrite precipitations than in the head and web of the rail. The grain number is 8. At a distance of 5 mm from the joint line (Figure 4, *d*) the grain number is 6-7. In the zone of a partial recrystallization, at a distance of 32 mm from the joint line, the microstructure is insignificantly different from that of the rails R65 after HT. The grain number is 7-8.

The hardness of the base metal of rails UIC60 in the head is *HRC* 35, in the web and flange it is *HRC* 30. After welding, the investigated joints differed by a sharp decrease in hardness *HRC* along the joint line (Figures 5, 6) from the level of the base metal, in the head to *HRC* 13, in the flange to *HRC* 15. In the zone of a coarse grain, at a distance of 5 mm from the joint line, the hardness was at the level of the base metal. In the zone of a partial recrystallization, located at a distance of 18–22 mm from the joint line, the hardness in the head is *HRC* 26, in the web and flange is *HRC* 23–25. After HT of welded joints, the deviation of hardness decreased. Along the joint line in the rail head the hardness is *HRC* 24, in the flange it is *HRC* 24. At a distance of 4–6 mm from the joint line and up to the zone of a partial recrystallization, the hardness in the head is *HRC* 34–35, which cor-

Table 2. Grain number of metal of welded joints of rails UIC60 after welding and after HT

Rail element	Grain number after welding			Grain number after HT			Base metal
	Joint line	5 mm from the joint line	Zone a partial recrystallization	Joint line	5 mm from the joint line	Zone a partial recrystallization	
Head	2-3	4-5	7-8	8	6-7	7	5-6
Neck	3-4	5	9-10	8	7	7-8	5-6
Foot	3-4	4-5	9-10	8	6	7-8	5-6

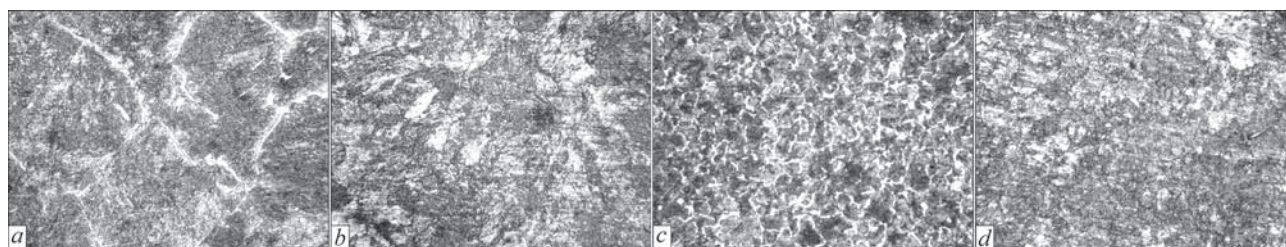


Figure 4. Microstructure ($\times 500$) of metal of welded joints of rails UIC60: joint line (a, c); at a distance of 5 mm from the joint line (b, d); after welding (a, b); after HT (c, d)

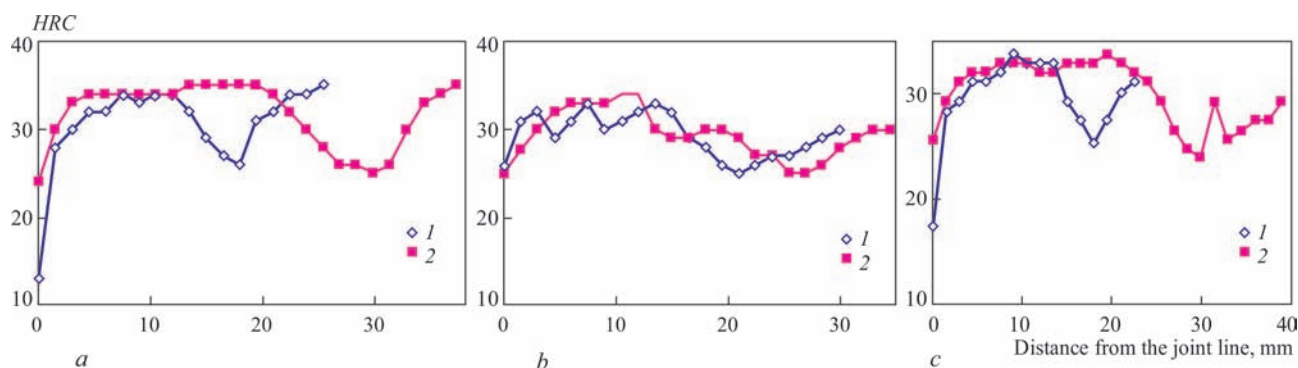


Figure 5. Distribution of hardness along the width of HAZ of welded joints of rails UIC60 in the head (a), in the web (b) and in the flange (c); after welding (1) and after HT (2)

responds to the level of base metal. At a distance of 18–22 mm from the joint line (zone of a partial recrystallization after welding), the hardness in the head increased to the level of base metal. In the zone of a partial recrystallization, the decrease in hardness did not differ from that of joints after welding.

In the rail head, the deviation in the hardness HRC from the level of base metal (Figure 6) decreased from 63 % (after welding) to 30 % (after HT). In the zone of a coarse grain, at a distance of up to 30 mm from the joint line, the hardness deviation decreased from 8 to 3 %. In the zone of a partial recrystallization, the deviation of the hardness HRC is 25 % after welding and after HT.

Conclusions

1. In the portable module of PWI for HT of welded joints of railway rails, the use of inductors with magnetic cores and technology of induction heating by currents of 2.4 kHz frequency provides a uniform distribution of the temperature field in welded joints, a low temperature drop between the surface and deep layers of the rail, as well as shortening in heating time.

2. As a result of HT of welded joints of rails R65 of steel K76F and rails UIC 60 of steel 900A in the portable module of PWI, the microstructure of metal of the welded joints is significantly changed, the hardness HRC is uniformly distributed over the width of the HAZ, the deviation of the hardness HRC from the level of base metal is decreased.

1. Genkin, I.Z. (2003) Heat treatment of rail welded joints in induction units. *The Paton Welding J.*, **9**, 38–41.

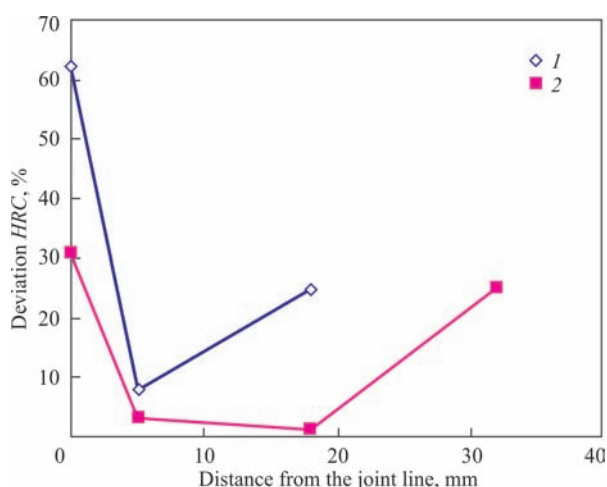


Figure 6. Deviation of hardness HRC in the head of the rails UIC60 after welding (1) and after HT (2)

2. Nesterov, D.K., Sapozhkov, V.E., Levchenko N.F. et al. (1990) Heat treatment of rail steel using induction heating. *Metallovedenie i Term. Obrabotka Metallov*, **8**, 30–34 [in Russian].
3. Feshchukov, A.N. (2016) *System for heat treatment of rail welded joints in track conditions*. Pat. 57752 RF, Int. Cl. E01B31/18 [in Russian].
4. Rezanov, V.A., Fedin, V.M., Bashlykov, A.V. et al. (2013) Differentiated hardening of rail welded joints. *Vestnik VNIIZHT*, **2**, 28–33 [in Russian].
5. Fedin, V.M., Zeman, S.K., Borts, A.I., Nikolin, A.I. (2005) Development of new technological equipment for restoration of used rails. *Ibid.*, **4**, 22–25 [in Russian].
6. Panteleymonov, S.O. *Complex for heat treatment of rail welded joints in track conditions*. Pat. 114593 Ukraine, Int. Cl. E01B31/18; 10.03.2017 [in Ukrainian].
7. Panteleymonov, E.A., Gubatyuk, R.S. (2016) Induction device for heat treatment of welded joints of railway rails. *The Paton Welding J.*, **9**, 41–43.

Received 01. 01.2018

AC ARC STABILIZER FOR WELDING TRANSFORMERS

V.V. BURLAKA, S.V. GULAKOV and S.K. PODNEBENNA

SHEI «Priazovskii State Technical University»

7 Universitetska Str., 87500, Mariupol, Donetsk Reg., Ukraine. E-mail: office@pstu.edu

Circuit design of AC arc stabilizer for welding transformers is proposed. A special feature of the stabilizer is application of resonance voltage rise in the transformer secondary winding to ensure repeated ignitions of the arc after each zero current transition. This allows reducing energy losses in the arc stabilizer and ensuring effective formation of high-voltage pulse packets for guaranteed breakdown of the arc gap. Application of the proposed arc stabilizer allows performance of DC welding with electrodes at power supply from welding transformers without rectifiers. The stabilizer is designed for operation with transformers not fitted with electronic regulators: mainly with transformers with a magnetic shunt of TDM, STSh type. 12 Ref., 6 Figures.

Keywords: *electric arc, welding, arc ignition, arcing stabilization, welding transformer, arc ignition voltage*

In manual arc welding the process quality and productivity are affected by the ability of the power source to provide easy ignition and stable burning of the arc. In AC welding arc reignition should occur after each zero transition of welding current. Devices for arcing stabilization or arc stabilizers are used for this purpose.

Arc ignition is associated with the need to generate high voltage. This can be achieved through application of additional windings of the welding transformer [1]; special circuits with additional inductive components which are connected in parallel [2] or in series with welding transformer secondary winding [3–8].

The first approach requires changing the transformer design and is not suitable for modification of the available park of welding transformers.

Realization of the second approach leads to greater overall dimensions and weight of arc stabilizer in connection with availability of additional inductive components, particularly those that are included into the welding circuit in series with the transformer secondary winding.

An original approach to creation of arc stabilizers is application for arc reignition of the energy which can be accumulated in the stray field of welding transformer. Considering that welding transformers usually have a falling output characteristic and greater scatter, such an approach seems promising.

References [9, 10] describe AC arc stabilizer, which is connected to the terminals of welding transformer secondary winding and contains an electronic switch, connected to this winding, and switch control circuit.

The circuit enables igniting the arc after zero transition of the mains voltage, and reigniting the arc in the case of its breaking; contains no power inductive components, and has simple connection. The disadvantages of this circuit are the impossibility to form out-

put voltage pulses of higher frequency, as at a failed attempt of arc gap breakdown, the energy stored in the welding transformer magnetic field is scattered in the form of heat on overvoltage protection elements of the electronic switch. That is why increase of output pulse frequency will lead to overheating of switch protection elements. Moreover, the high rate of output voltage change leads to generation of radio frequency noise. This impairs the consumer properties of arc stabilizer.

The authors improved AC arc stabilizer [11] that allowed reducing energy losses in it, increasing the duration of the period of maintaining higher voltage at the electrode at manual arc welding and facilitating the process of arc initiation, thus improving the consumer characteristics and widening the device application field. Moreover, a variant of the device was created [12], which has increased output voltage without the need to apply power components with increased working voltage.

The idea consists in connecting a capacitor to secondary winding of welding transformer. The capacitor forms an oscillatory circuit together with transformer leakage inductance. Connected in parallel to this capacitor are electronic keys with the control circuit that ensures «pumping» of the circuit with energy. This leads to voltage increase on the capacitor and welding source output.

Simplified circuit of power components of the device for AC arc stabilization that implements the described principle is given in Figure 1.

Formation of higher voltage of arc initiation is realized at the expense of pumping the resonant loop formed by T1 and C_R elements.

VD1, S1 elements operate in positive halfwave of secondary voltage of welding transformer T1 (S1 is switched, S2 is switched off), VD2, S2 elements operate in negative halfwave (S2 is switched, S1 is switched off).

We will consider the process in the positive halfwave.

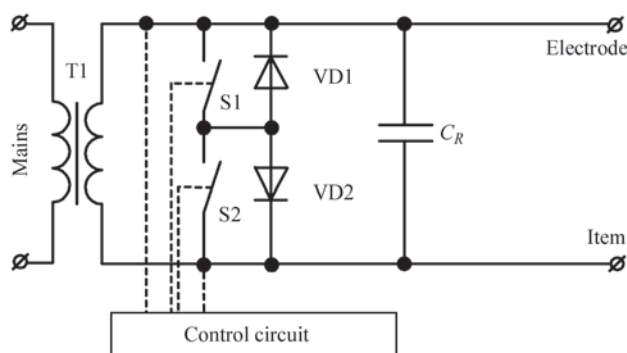


Figure 1. Schematic of power components of the device for AC arc stabilization

Key S1 opens immediately after zero transition of T1 secondary voltage. Figure 2 gives voltage oscillogram at capacitor C_R in this mode. Energy storing in T1 leakage inductance begins. As soon as current of key S1 has reached the set «pumping» current (this current determines the amplitude of output voltage and discharge energy), control system closes S1 (moment of time t_1). Resonance charging of capacitor C_R starts. After a quarter of the period of resonance frequency of the circuit formed by leakage inductance T1 and capacitor C_R , the latter is charged up to maximum voltage, and the current drops to zero. C_R discharge to T1 begins. After a half-period of resonance frequency the voltage at C_R goes through zero and becomes negative, and current reaches its minimum value. Control system opens S1 at appearance of negative voltage at C_R (moment of time t_2). This, however, does not influence the process, as diode VD2 is closed by reverse voltage.

After three-fourths of resonance frequency period voltage at C_R reaches a minimum, and current approaches zero. C_R charging from T1 secondary winding begins. When voltage on C_R goes through zero and becomes positive, winding current will flow through diode VD2 and pre-open key S1 (moment of time t_3). Additional «pumping» of the inductance up to set current will occur, which will be followed by S1 closing (moment of time t_4), and the process will be repeated. S1 switching is «soft», as it is opened at

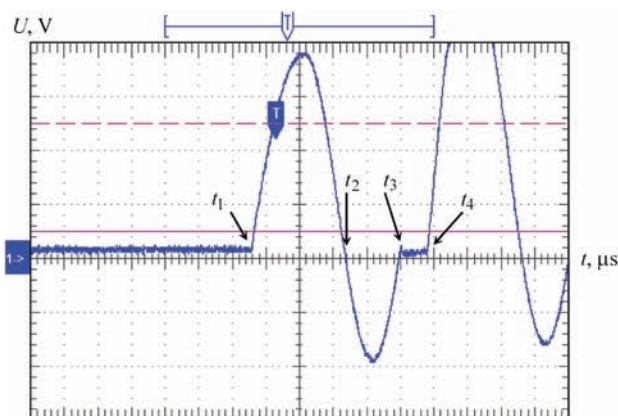


Figure 2. Oscillogram of voltage at capacitor C_R (voltage at transformer secondary winding) (8 $\mu\text{s}/\text{div}$; 50 V/div)

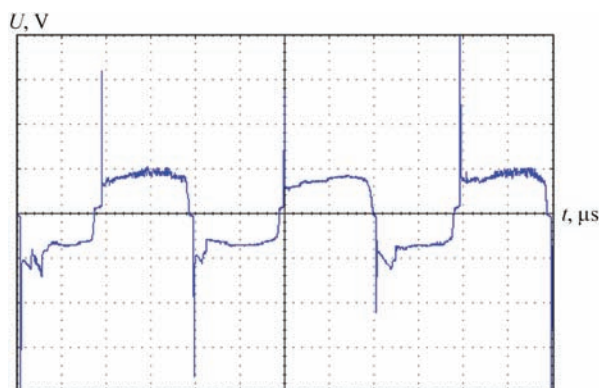


Figure 3. Oscillogram of voltage at transformer secondary winding during welding (5 $\mu\text{s}/\text{div}$; 50 V/div)

negative voltage at C_R (when VD2 diode is closed), and its closing occurs at voltage close to zero at C_R , that is the rate of voltage rise at S1 is limited by C_R action. At negative halfwave of T1 secondary voltage all the processes proceed in a similar fashion.

Two scenarios are possible during circuit operation: arc initiation occurs at certain voltage at C_R . Here, voltage at the output of arc power source decreases to the value of arc voltage across the arc gap, control system blocks operation of keys S1, S2 till the next zero transition of voltage of T1 secondary winding. This provides «soft» ignition and stabilization of the arc; if voltage at C_R becomes too high, the control circuit lowers the current of «pumping» resonant loop T1- C_R and the system goes into the steady-state mode.

During arcing, capacitor C_R does not have any significant influence on the process, because of its low capacity. Arc initiation occurs after each zero transition of secondary voltage of welding transformer.

The authors have made arc stabilization devices using the proposed engineering solution. Stabilizers were installed in TDM-401 and STSh-250 transformers, and their industrial testing was performed during repair operations at metallurgical enterprises of the city of Mariupol. Welding transformers fitted with arc stabilizers were used for DC welding with UONI type electrodes.

Stabilizer control system is based on single-crystal microcontroller and supports the following functions: identification of arc burning by the results of analysis

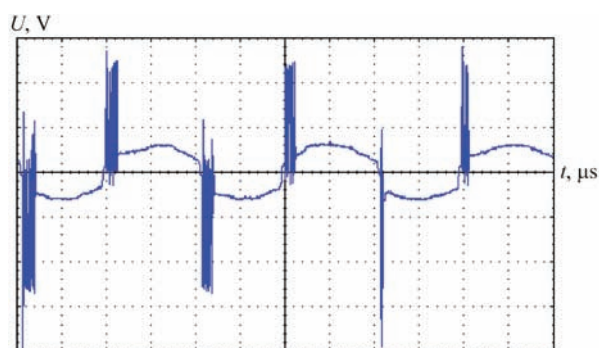


Figure 4. Oscillogram of voltage at transformer secondary winding during welding, one can see packets of arc ignition pulses (5 $\mu\text{s}/\text{div}$; 50 V/div)

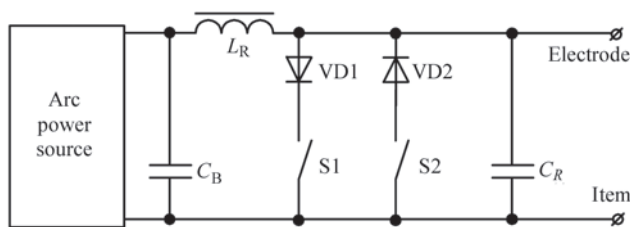


Figure 5. Circuit of power components of arc stabilization device with resonant choke

of transformer secondary voltage; stabilization of arc ignition voltage; automatic adjustment for transformer parameters; limiting the time of action of increased voltage at a failed attempt at arc initiation; thermal protection of power elements of the circuit.

Figures 3, 4 show oscillograms of secondary voltage of TDM-401 welding transformer with a connected arc stabilizer at manual arc welding with UONI-13/55 electrodes. One can see that situations arise (Figure 4), when arc reignition proceeds not immediately, but after several increased voltage pulses. Amplitude of arc reignition pulses reaches 200 V, and at initial arc ignition (after electrode closure on the item) it can be up to 300 V. Stabilizers showed stable operation in the entire range of regulation of welding current of transformers with a magnetic shunt.

The proposed arc stabilizer is suitable for operation with welding transformers, not fitted with electronic devices of welding current regulation, as appearance of high voltage of the frequency of tens of kilohertz in the transformer secondary winding can lead to violation of the mode of electronic regulator operation.

The authors developed a version of arc stabilizer with a two-wire connection to the transformer, that is power to the control system is supplied from secondary voltage. Overall dimensions of such an arc stabilizer are just 110×90×48 mm.

If the Q-factor of welding transformer leaves much to be desired, or it is undesirable to apply higher frequency high voltage to its secondary winding, it is rational to fit the arc stabilizer with a separate resonant choke with known characteristics, and install high-frequency blocking capacitor in parallel to transformer secondary winding. This, certainly, impairs the technical-economic and mass-dimensional parameters of the stabilizer, as it acquires a power inductive component. Figure 5 gives the schematic of power part of such a variant of arc stabilization device.

The device is connected between the arc power source and welding electrode, includes resonant choke L_R of blocking capacitor C_b and resonance capacitor C_R , electronic keys S1, S2 and two diodes VD1, VD2. The keys can be connected also as shown in Figure 1, circuit functionality remaining the same.

For TIG welding keys S1, S2, diodes VD1, VD2 and capacitor C_R should be designed for higher volt-

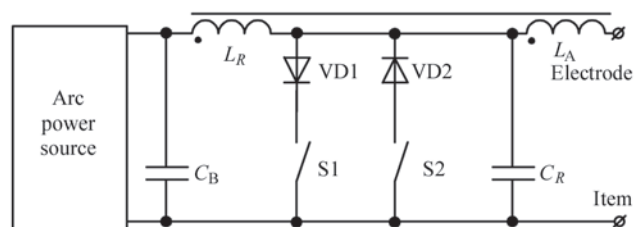


Figure 6. Power part of arc stabilization device with higher voltage, as increased voltage of arc ignition should be provided for TIG process, compared to manual arc welding. Moreover, for TIG welding the choke can be made with additional winding (L_A , Figure 6), which is connected in series with the main one.

Such «autotransformer» connection of the choke allows obtaining higher output voltage without the need to replace the force components by higher voltage ones. With correct design of the choke parameters, voltage with amplitude of several kV can be obtained at the electrode that can be used for contactless arc ignition in TIG welding.

- Zaruba, I.I., Andreev, V.V., Dymenko, V.V. (2001) Improvement of transformers for manual arc welding. *The Paton Welding J.*, **3**, 43–46.
- Andrianov, A.A., Sydorets, V.N. (2009) Optimization of modes of stabilization of alternating current welding arc. *Elektrotehnika i Elektromekhanika*, **2**, 5–8 [in Russian].
- Makhlin, N.M., Korotynsky, A.E. (2014) Analysis and procedure of calculation of series connection electronic devices for contactless arc excitation. *The Paton Welding J.*, **1**, 30–40.
- Makhlin, N.M., Korotynsky, A.E. (2015) Asynchronous exciters and stabilizers of arc. Analysis and calculation procedure. Pt. 1. *Ibid.*, **3–4**, 24–35.
- Makhlin, N.M., Korotynsky, A.E. (2015) Asynchronous exciters and stabilizers of arc. Analysis and calculation procedure. Pt. 2. *Ibid.*, **7**, 26–37.
- Makhlin, N.M., Korotynsky, O.E., Skopyuk, M.I. (2014) *Device for excitation and stabilization of alternating current arc burning process*. Pat. 109334 Ukraine. Int. Cl. B23K 9/067 (2006.01); B23K 9/073 (2006.01); No. a 2014 00292 [in Ukrainian].
- Burlaka, V.V., Gulakov, S.V. (2016) Device for excitation and stabilization of welding arc. *The Paton Welding J.*, **11**, 43–46.
- Burlaka, V.V., Gulakov, S.V. (2016) *Device for arc stabilization*. Pat. 115200 Ukraine. Int. Cl. B23K 9/067 (2006.01); B23K 9/073 (2006.01); No. a 2016 08174 [in Ukrainian].
- Zaruba, I.I., Andreev, V.V., Shatan, A.F. et al. (2012) New type of pulse stabilizer of alternating current welding arc. *The Paton Welding J.*, **2**, 43–45.
- Paton, B.E., Zaruba, I.I., Andreev, V.V. et al. (2011) *Device for initial and repeated welding alternating current arc ignition*. Pat. 62596 Ukraine. Int. Cl. B23K 9/00 (2011.01); No. u 2020 14476 [in Ukrainian].
- Burlaka, V.V., Gulakov, S.V. (2017) *Device for stabilization of alternating current arc*. Pat. 114990 Ukraine. Int. Cl. B23K 9/067 (2006.01); B23K 9/073 (2006.01); No. a 2016 067 [in Ukrainian].
- Burlaka, V.V., Gulakov, S.V. (2017) *Stabilizer of alternating current arc*. Pat. 114998 Ukraine. Int. Cl. B23K 9/067 (2006.01); B23K 9/073 (2006.01); No. a 2016 08173 [in Ukrainian].

Received 12. 01.2018

Poland Institute of Welding in Gliwice



Building of Welding Institute in Gliwice

The Poland Institute of Welding has started its operation in a period directly after the end of the Second World War. The Institute was founded in 1945, and its first task was training of gas- and electric welders, which were desperately necessary for the country ruined as a result of war.

Since 1949 the Institute started to be transformed into a scientific-and-research organization. The first research departments were created. They solved the problems in the field of welding technologies, weldable materials and consumables.

The deciding step in the Institute development was formation in 1954 a department on design of welding and auxiliary equipment as well as department of prototypes of welding equipment. After the war the material resources of welding engineering in Poland included only one plant on welding electrode production, one factory on manufacture of gas welding equipment and several tens of enterprises on production of oxygen and acetylene. There was no production of electric equipment for welding at all and the most widespread method of joining in manufacture of heavy steel structures (boilers for power engineering, vessels, ships, bridges) was riveting.

Both departments were located in the Institute premises. Their first achievements were development of a series of pressure resistance welding machines of 2, 6 and 10 kV·A power for wires and acetylene vessel valves as well as 500-ampere welding transformer based on Soviet sample of that period. Two years later both departments were joined in one titled a department on welding equipment production (ZBUS), which designed and developed the prototypes of welding equipment, machines, automatic machines and apparatuses necessary for functioning and development of welding engineering in Poland. Replicated and improved prototypes were sent into serial production at commercial enterprises created in Poland. The examples of the first prototypes are welding transformers, welding power sources based on internal combustion engines, high-pressure acetylene generators, automatic machines for electroslag welding, semi-automatic machines for oxygen cutting, machines for resistance butt welding of rods and tubes, oxygen reducing units including mains ones, flux collectors, devices for welding wire winding and many others.

Due to systematic and purposeful work, all the conditions were created in the Institute for successful development of modern welding engineering in Poland. At the end of 1958–1959 the Institute had an effective system of training and education of welding staff, department on design and manufacture of welding equipment, a team of researches carrying multiple investigations in the field of welding as well as the whole complex of premises and laboratories equipped with not bad equipment and apparatuses for researches. In this period the leaders of the country after carrying the evaluation of work of industrial research centers, took a decision that the Welding Institute should keep the status of the research institute.

The Institute has been carrying multiple, very interesting and quite often complex research works since 1960. Different welding equipment was also developed and manufactured in great volumes.

A bright example can be a flow line, including 12 welding automatic machines, for automatic welding of walls of coal vessel carriages at wagon works. The line was implemented in industry in 1962. The Institute organized the conferences and meetings of the welding specialists, during which the Institute staff presented their reports. It was the period when the first foreign business trips took place, including for participation in the congresses of the International Institute of Welding, in which the Welding Institute in Gliwice is the official representative of Poland since July 1, 1956.

The next expansion of the Institute took place in a period of 1966–1968. Earlier existing and constructed close to them buildings have been modernized a lot of times after that, but they are successfully used in that layout and size up to the moment.

In 1968 the Institute was the organizer of the XXI Congress of the International Institute of Welding. The chairman of Organizing Committee was Prof. Jozef Pilarczyk, the main founder of the Institute in 1945 and its Director for many years. In 1967 Prof. Jozef Pilarczyk decided to concentrate only on activity of a welding chair of the Silesian University of Technology as its leader, keeping at that the position of the chairman of Scientific Council of the Welding Institute.

A lot of new had appeared in the 1970th. In this period Poland got the foreign credits, which in addition to other was used for construction of many modern for that time enterprises as well as promoted significant technological progress. A series of new methods of fusion and pressure welding appeared in the field of welding engineering and the Institute intensively worked with them. The investigations were carried out on CO₂ welding, then in gas mixtures, plasma welding and cutting, electroslag and electrogas welding, friction welding, mechanized and automatic thermal cutting etc. In parallel a wide spectrum of investigations was carried out in the field of weldability of a series of modern structural steels, which were manufactured by Poland metallurgical industrial complexes, as well as consulting services and surveillance of performance of critical welded structures was provided when realizing large investment programs. Multiple stations and lines for mechanized welding and cutting were developed and implemented in commercial production. Significant changes also took place in the field of science due to funding of large research projects within five-year periods directed on so-called key problems (later on Central Research Programs) covering a wide topics of the whole branches. The Institute actively participated in these programs realizing.

An important event in the Institute live was organizing and realizing in cooperation with the Silesian University of Technology the carrier enhancement courses for welder-engineers. The lectures and practical activities for course listeners took place in the Institute premises and the staff members of the Institute with rich scientific and production experience performed duties of the trainers. The courses were hold during 10 years till 1980.

The 1980th were difficult years in the Institute live. A martial law declared in Poland on December 13, 1981, heavy social and political situation, dramatic reduction of commercial production, loss and break of connections, dismissal of large amount of staff members, retirement or termination on health grounds, all these result in the fact that the work in the Institute was performed with jerks, irregularly, and financial situation was very bad that adversely affect low salaries and absence of investments for development. Staff problems were also great, which were explained by absence of young engineers. The consequences of this situation was observed for a long time since in a course of several years the Institute was lack of staff members brought up in the Institute and inspired by its patriotism.

Regardless the difficulties in 1981–1985 the Institute continued coordination of the key problem «Methods and means of mechanization and automaton of welding works» and in 1986–1990 the Central Scientific-Research Program «Welding technologies». Together with the Institute all the most significant scientific-and-research Poland centers working in the field of welding were engaged in these programs realizing.

The Institute has started functioning in completely new conditions since 1990. In 1989 Poland turned to the way of free development and passed from center-controlled low-effective socialistic economy to competitive market economy. Everyone was dreaming about such changes, however, not everybody realized the principal difference between the life in modest, but nevertheless socially guaranteed conditions of socialist state, and life probably on higher level under market economy conditions, that, though was related with heavy and responsible every day work.

In 1990 the Institute was the innovative institute. The same year a decree about such enterprises was published. It provided them larger freedom of action, but simultaneously formed the grounds for complete self-financing and responsibility for taken decisions. Thus, the funds stopped arriving on the Institute accounts for their functioning and corresponding ministries providing in the last vital activity and surveillance over these organizations, remained only as their founders. A lot of scientific-and-research institutes couldn't survive under such new conditions.

The changed decree on the innovative institutes indicated that new director would not be appointed anymore, but should be selected for a position by running a competition, besides the period was not unlimited anymore, but made 5 years. The Director should express the agreement to take up the position not by order, but

based on his/her own choice with complete understanding that the destiny of the Institute is determined based on his/her individual decisions.

As a result of first in the history carried competition the Director of the Institute on November 1, 1990 became Prof. Jan Pilarczyk, son of Prof. Jozef Pilarczyk. The Institute started rapidly adapting to new situation passing the difficult way from flexible transformation and work in accordance with the principles of free competitive market. Big rearrangement of the Institute covered the organization structure, personnel, activity topics, available equipment and condition of the premises.

The Institute buildings constructed in a period from 1945–1970 were fundamentally modernized in 1990–2015 and got a new modern appearance and were filled with state-of-the art apparatuses and equipment. All the elements of Institute infrastructure were also repaired. New staff, which could work on new principles taking into account new requirements, was searched.

The Institute intensified its activity directed on development and improvement of different methods of welding and welding technologies, structural materials, welding consumables and equipment as well as made the new steps, exclusively in the field of welding, bringing income to the Institute. Among them are training of welding personal in accordance with national and European programs, surveillance of welding education in Poland, evaluation and certification of the enterprises producing welded structures, performance of the tests in certified and accredited laboratories, examination and qualification of welding technologies, certification of welding products, personal and quality systems, development of PN-EN standards, implementation in practice the rules and legal acts as well as elaboration of instructions and requirements. Simultaneously, the Institute stopped development and implementation in commercial production of welding equipment, stations and production lines for mechanized and automated welding and cutting. Professional welding companies, Poland and foreign ones, which stated to appear in Poland, became engaged in these matters.

The main task of the Institute. i.e. work in accordance with the principles and requirements of the free market, was expanded by no less important second task, namely rearrangement of Institute functioning taking into account European standards. European Union was formed in 1992 and Poland got the status of observer-state. A series of European organizations appeared in scope of the Union. One of them was the European Welding Federation (EWF). The main task of the Federation was creation of the single system of training and education of welding personnel recognized by all partners. The system was then distributed due to cooperation with the International Institute of Welding in the countries out of the European Union borders, and in 2001 was recognized as a global system for welding staff training. The Welding Institute as an exclusive body in Poland was included in a harmonized system for education, testing, qualification and certification of welding personnel and had the right to issue European and international diplomas and certificates to the enterprises and welding staff. Several thousand of such documents have been issued up to the moment. They allow enterprises to function in European market and struggle for receiving export contracts.

On October 1, 2010 the Institute changed the status from «innovative» to «research». It became possible due to acceptance of a new decree on research institutes.

The Institute is equipped with very good level modern equipment and apparatuses, which are not inferior to similar in the welding institutes all over the world. The Institute has got up-to-date equipment for arc welding, very good lasers with wide spectrum of possibilities for performance of welding, cutting and many other related processes, new unit for electron beam welding, machines for modern pressure welding by all methods, equipment for brazing and, besides, wide spectrum of reference and measurement devices as well as unit and software for welding thermal cycles simulation. The Institute has good data base, which was developed in course of last decades, and creates good working conditions for all members of the Institute providing direct contact with all the most important clients and external partners.

The Institute realizes a series of research projects in cooperation with the National Research Center and National Science Center as well as many industrial partners and foreign research centers. After more than 70 years of active work, the Welding Institute in Gliwice can be proud of a series of meaningful achievements. Such a progress in the research departments, laboratories and centers of the Institute were received due to fruitful and self-denying work of several generations of the Institute staff.

Prof. Jan Pilarczyk

WELDING OF TITANIUM

AND ITS ALLOYS

A team of experts in the field of welding of titanium and alloys on its basis has been working at PWI for more that 30 years. For the first time in the world the unique technologies of non-consumable argon-arc welding of titanium with halogenide fluxes; narrow-gap argon-arc tungsten electrode welding with controlling magnetic field; press welding of titanium with copper and aluminum with steel were developed in course of these years.

The technologies for titanium and its alloys welding developed at the PWI have found wide application in aircraft- and rocket construction as well as at enterprises of chemical machine building of CIS countries. Currently, PWI fulfills contract-based complex works on development of technology and equipment for titanium welding and engineering maintenance at manufacture of specific products.



Developed by the E.O. Paton Electric Welding Institute of the NAS of Ukraine. E-mail: office@paton.kiev.ua

MICROPLASMA SPRAYING

OF BIOCOMPATIBLE COATINGS ON IMPLANTS

PWI has developed a technology and equipment of microplasma spraying of biocompatible coatings on the surface of different implants, including hip implants, dental implants, intervertebral cages etc.

This technology allows depositing coatings from hydroxyapatite powder (HA), titanium cellular coatings as well as double-layer biocermet (titanium-hydroxyapatite) coatings. Spraying of biocompatible coatings is done on microplasma spraying unit MPN-004. PLASMATRON FOR SPRAYING OF COATINGS
Pub. No.:WO/2004/010747, International Application No.: PCT/UA2003/000014, Publication date: 29.01.2004. (IRP4).



Unit for microplasma spraying MPN-004 with powder batchbox

Spraying of Ti-layer with regulated porosity (5–30 %, pore size 50–300 μm) and minimum oxidation level is carried out by means of microplasma spraying of Ti-wire. Combination of cellular Ti-coating with external HA layer provides coating cohesion strength with implant surface satisfying ISO 13779-2 and high level of biocompatibility.

- > Based on complete complex of mechanical and biomedical tests the implants with microplasma biomedical coatings are used in practice for hip replacement.



a



b



c

Products with biocompatible coatings made by microplasma spraying: *a* — parts of hip implant; *b* — cermet implant for interbody spinal fusion; *c* — dental implant

Developed by the E.O. Paton Electric Welding Institute of the NAS of Ukraine. E-mail: office@paton.kiev.ua

PATON PUBLISHING HOUSE

www.patonpublishinghouse.com

SUBSCRIPTION

The Paton
WELDING JOURNAL

АВТОМАТИЧЕСКАЯ
СВАРКА

«The Paton Welding Journal» is Published Monthly Since 2000 in English, ISSN 0957-798X, DOI: <http://dx.doi.org/10.15407/tpwj>.

«Avtomaticheskaya Svarka» Journal (Automatic Welding) is Published Monthly Since 1948 in Russian, ISSN 005-111X, DOI: <http://dx.doi.org/10.15407/as>.

«The Paton Welding Journal» is Cover-to-Cover Translation of «Avtomaticheskaya Svarka» Journal into English.

If You are interested in making subscription directly via Editorial Board, fill, please, the coupon and send application by Fax or E-mail.

The cost of annual subscription via Editorial Board is \$348 for «The Paton Welding Journal» and \$180 for «Avtomaticheskaya Svarka» Journal.

«The Paton Welding Journal» can be also subscribed worldwide from catalogues subscription agency EBSO.

SUBSCRIPTION COUPON

Address for journal delivery _____

Term of subscription since _____

20

till

20

Name, initials _____

Affiliation _____

Position _____

Tel., Fax, E-mail _____

We offer the subscription all issues of the Journals in pdf format, starting from 2009.

The archives for 2009–2016 are free of charge on www.patonpublishinghouse.com site.



ADVERTISEMENT

in «Avtomaticheskaya Svarka» and «The Paton Welding Journal»

External cover, fully-colored:

First page of cover
(190×190 mm) — \$700
Second page of cover
(200×290 mm) — \$550
Third page of cover
(200×290 mm) — \$500
Fourth page of cover
(200×290 mm) — \$600

Internal cover, fully-colored:

First/second/third/fourth page
of cover (200×290 mm) — \$400

Internal insert:

Fully-colored (200×290 mm) — \$340
Fully-colored (double page A3)
(400×290 mm) — \$500

- Article in the form of advertising is 50 % of the cost of advertising area
- When the sum of advertising contracts exceeds \$1001, a flexible system of discounts is envisaged

Size of journal after cutting is 200×290 mm

Editorial Board of Journals «Avtomaticheskaya Svarka» and «The Paton Welding Journal»

E.O. Paton Electric Welding Institute of the NAS of Ukraine

International Association «Welding»

11 Kazimir Malevich Str. (former Bozhenko Str.), 03150, Kiev, Ukraine

Tel.: (38044) 200 60 16, 200 82 77; Fax: (38044) 200 82 77, 200 81 45

E-mail: journal@paton.kiev.ua; www.patonpublishinghouse.com